CECAM 2027 HeDFT Tutorial "Dopant Dynamics in Superfluid Helium-4 Nanodroplets: from Statics to Time-Dependent He-DFT", Lecture Notes.

Density Functional Theory of Superfluid Helium and Droplets

J. Navarro[1] and M. Barranco[2]
[1]IFIC-CSIC, Valencia (Spain)
[2]University of Barcelona, Barcelona (Spain)

June 24, 2017

Contents

The present lecture notes are devoted to the topic of Density Functional Theory in helium systems. They are not intended to be a review of the subject, but rather a pedagogical introduction to it. The main objectives are to provide the readers with an elementary introduction to the physics of liquid helium, and to discuss the use of Density Functional methods to study ^{4}He bulk liquid and droplets. We thus exclude many other interesting systems and topics such as helium films, cavitation in liquid helium, two- and one-dimensional systems, atomic and molecular impurities, vortices... These subjects are discussed in two recent reviews on the DFT approach to liquid helium and droplets [1, 2], and in some notes describing the practical implementation of DFT for liquid helium systems [3]. Actually, the present notes aim at complementing to some extent those references by discussing basic aspects of the physics of liquid helium and of the DFT approach not discussed in [1, 2, 3].

The plan of these lectures is the following. In Section 1 some general properties of liquid helium are presented to introduce the non familiar reader with the topic. A minimum of phenomenology is given to build up useful DFT. In Section 2 the DFT formalism is discussed in the form of the Hohenberg-Kohn theorem and the Kohn-Sham scheme. Systems such as atomic nuclei and liquid helium are characterized by a strong short-range repulsion, and an almost completely phenomenological DFT is required from the very beginning. Finally, Section 3 is devoted to the explicit construction of these DF for helium-4 systems.

As useful references on liquid helium and droplets we mention the books by Wilks and Betts [4], and Glyde [5], and to the collection of papers in [6]. As for the ^{3}He isotope, not discussed in the present lectures, we refer to the book by Dobbs [7] and to the chapter by Hernández and Navarro in [6]. Finally, concerning density functional theory, we refer to the original papers by Kohn and collaborators [8, 9] and to the book by Dreizler and Gross [10].

1 The Physics of Liquid Helium

Helium was discovered in the solar crown during an eclipse in 1869, and in terrestrial uranium minerals in 1895. Kammerlingh Onnes succeded its liquefaction in 1908, cooling the gas down to 5.2 K. At the scale of Universe, matter is mostly formed by hydrogen ($\approx 75\%$) and helium ($\approx 25\%$), but these proportions are very different on Earth. In particular, helium represents only 5×10^{-4} % in the atmosphere and $\simeq 10^{-6}$ % in the crust. Helium is the lightest element of the inert gases and has two stable isotopes ^{4}He and ^{3}He, the former being a 99.99986 % of the total population. The atomic structure of the helium atom is very simple: two electrons around a nucleus, with two protons and one neutron in the case of ^{3}He, and one more neutron in the case of ^{4}He. The ^{3}He atom is a fermion, as it contains an odd number of fermionic constituents, and has total spin 1/2. The ^{4}He atom, with an even number of fermions, is a boson of spin zero. The different statistical character of the two

helium isotopes produces dramatic differences in their physical properties. For that reason, in the next subsection we present results for both ^{4}He and ^{3}He isotopes.

1.1 Experimental miscellany

The experimental results shown in these notes can be found in Refs. [4, 11], where the original experimental references are cited. The phase diagrams of liquid ^{4}He and ^{3}He in the (P,T) plane at low temperature are shown in Fig. 1. Two remarkable facts can be noticed: i) both isotopes remain liquid down to the absolute zero temperature, ii) a "superfluid" phase transition (λ-line) takes place at 2.17 K for ^{4}He (at saturated vapor pressure) and 2.7 mK for ^{3}He (at about 33 atm). When the liquid is cooled below the transition temperature, its viscosity drops to almost zero and it is able to flow without dissipation through very narrow capillary tubes. Under these conditions, liquid helium not only is superfluid but also becomes a surprisingly good heat conductor.

In the following, ρ will represent the number density, that is, the number of helium atoms per volume unit. The usual equation of state of the liquid is the relation between pressure and density. Any microscopic theory starts by calculating the energy per particle E/N of the liquid at fixed density. Other interesting quantities are related to variations of the energy with respect to the volume (or, equivalently, to the number density). For instance, at $T = 0$, the pressure

$$P = -\frac{\partial E}{\partial \Omega} \equiv \rho^2 \frac{\partial E/N}{\partial \rho} \tag{1}$$

(Ω is the volume occupied by the liquid), the incompressibility modulus

$$K = -\Omega \frac{\partial P}{\partial \Omega} \equiv \rho \frac{\partial P}{\partial \rho} = \frac{1}{\kappa} \tag{2}$$

[κ is the compressibility modulus, $\kappa = -(d\Omega/dP)/\Omega$], and the related speed c of sound:

$$mc^2 = \frac{\partial P}{\partial \rho} = \frac{1}{\kappa \rho} \tag{3}$$

(m is the mass of the atom). The values of E/N, $P(\rho)$, $\kappa(\rho)$, and $c(\rho)$ are well known experimentally for both liquids at very low temperatures. In Fig. 2 are plotted the $T = 0$ extrapolation of the pressure and the speed of sound as a function of the number density ρ.

An important thermodynamical quantity which distinguishes in a crucial way ^{4}He from ^{3}He is the specific heat of the liquid, defined as $C_V = \partial \mathcal{E}(\rho)/\partial T$ at constant volume, where $\mathcal{E} = E/\Omega$. At low temperatures:

$$C_V(^4\mathrm{He}) \;=\; \frac{2}{15} \frac{\pi^2 T^3}{\rho (\hbar c)^3} \tag{4}$$

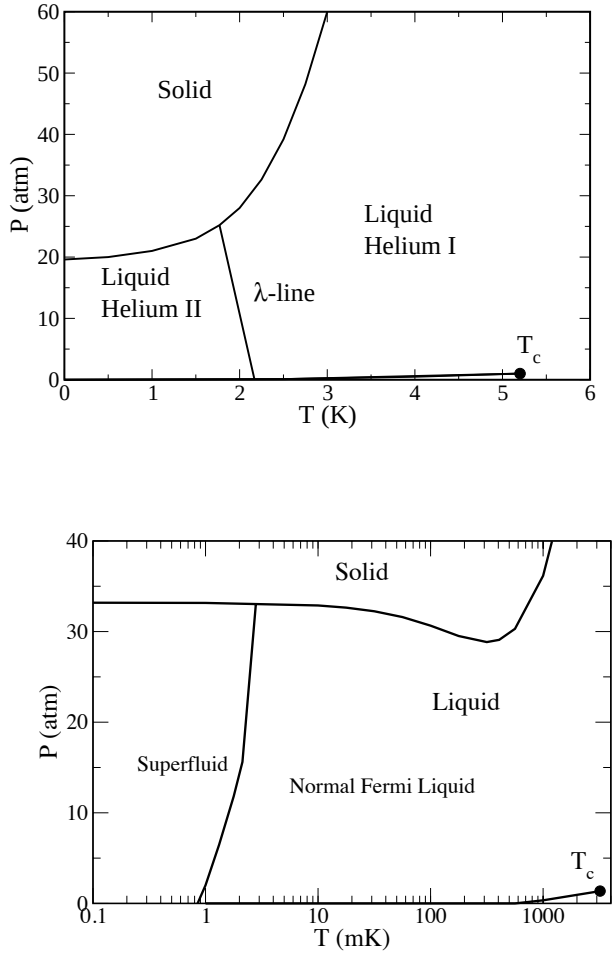

Figure 1: Schematic phase diagram of ^{4}He (top panel) and ^{3}He (bottom panel) in the (P,T) plane. Notice the logarithmic scale for the ^{3}He temperature.

$$C_V(^3\mathrm{He}) \;=\; \frac{1}{2}\frac{\pi^2 T}{\varepsilon_F^*} \tag{5}$$

The thermodynamical properties of liquid ^{4}He are characterized by the excitation of phonons. By contrast, the low energy excitations in ^{3}He are of single particle type, and the effect of the interaction appears through a renormalization of the mass, with

$$\varepsilon_F^* = \frac{\hbar^2 k_F^2}{2m^*} \tag{6}$$

the effective Fermi energy (this expression is valid at $T \ll \varepsilon_F^*$, and does not apply to the superfluid liquid ^{3}He). From measurements of C_V at several pressures one can extract the ^{3}He effective mass $m^*(\rho)$ as a function of the density, which is shown

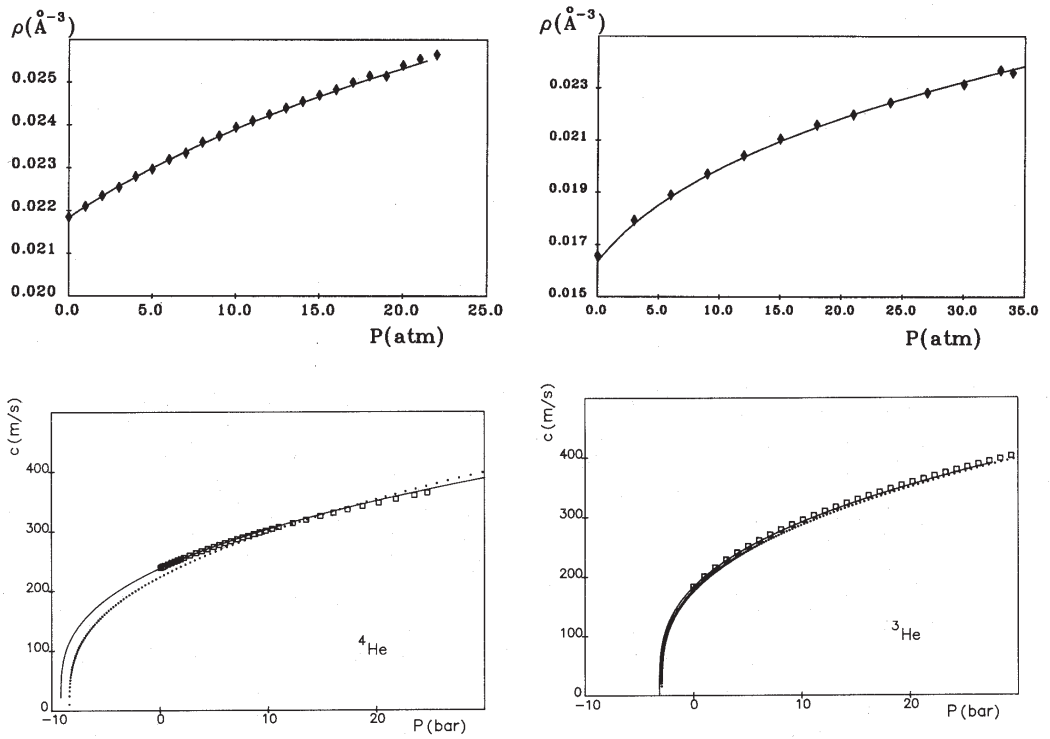

Figure 2: Equation of state (upper pannels) and speed of sound (lower pannels) of liquids ^{4}He and ^{3}He (left and right pannels, respectively). The solid lines are the results obtained with a density functional (see Sect. 3.1 for ^{4}He and Refs. [18, 20] for ^{3}He, and the dashed lines correspond to the results obtained as indicated in Ref. [21].

in Fig. 3. At saturation, the effective mass is almost three times the bare atomic mass. The physical meaning of such a renormalization involves the existence of spin excitations at small energies: one ^{3}He atom is surrounded by a cloud of spin excitations which increases its inertia. The consequence is a tendency to localize the atoms, thus reducing the zero-point motion.

Several characteristic properties of ^{4}He and ^{3}He are reported in Table 1, extrapolated to $T = 0$. Notice the units: lengths in Å (1Å $=10^{-10}$ m) and energies in K (1K $= 8.617 \times 10^{-5}$ eV $= 3.169$ μhartree $= 0.695$ cm^{-1}).

Some of these properties can be qualitatively understood taking into account that both isotopes feel the same interaction, but have different masses and statistics. The lighter mass of ^{3}He atoms translates into a larger mobility and therefore into a smaller saturation density as well as a smaller binding energy per particle. The volume per particle occupied by liquid ^{4}He is smaller than that of ^{3}He. Therefore, it is easier to compress liquid ^{3}He, and consequently the speed of sound in liquid ^{3}He is smaller than in liquid ^{4}He when they are compared at the corresponding

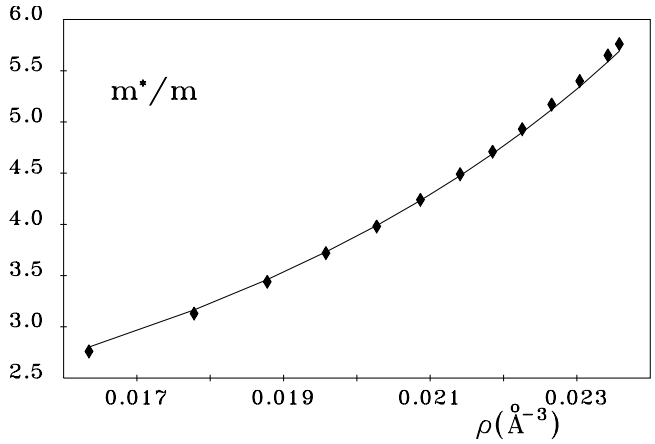

Figure 3: The ^{3}He atom effective mass in liquid ^{3}He. The solid line is the effective mass calculated with the density functional of Ref. [20]

Table 1: Characteristic properties of liquid heliums.

	^{4}He	^{3}He
$\hbar^2/2m$ (K Å^2)	6.0597	8.0418
ρ_0 (Å^{-3})	0.021836	0.016347
e_0 (K)	-7.15	-2.49
$1/\rho_0$ (Å^3)	46	61
$1/(\kappa_0\rho_0)$ (K)	27.3	12.1
c_0 (m/s)	238	183
$V_{\rm atom} \times \rho_0$	0.2	0.15
σ (K Å^{-2})	0.274	0.113
m_0^*/m	1	2.81

saturation densities. It is also worth noticing that the ratio of the volume occupied by each atom ($V_{\rm atom} = 4\pi R^3/3$ with $R \sim 1.3$ Å) to the available volume ($V = 1/\rho_0$) is approximately 0.2 for pure ^{4}He, thus indicating that the system is highly packed and that therefore the influence of correlations is strong (as a comparison, this ratio is about 0.05 for nuclear matter). The study of the free surface of the liquids has attracted many efforts for its relevance in the physics of quantum fluids. The surface tension σ at saturated vapor pressure of both ^{4}He and ^{3}He has been measured with high precision down to very low temperatures. Their values are more than 4 orders of magnitude smaller than that for water in normal conditions.

We finally mention that the existence of the ^{3}He-^{4}He mixtures permits the study of different types of excitations and the interplay of the correlations and statistics on the excitation spectrum, see Ref. [12] and references therein. Depending on the relative concentration, the resulting liquid may be a mixture or a coexistence of two

separate phases. ^{4}He or ^{3}He nanodroplets, either pure or mixed, allow to study the dependence of properties on the number of particles. Helium nanodroplets constitute a low temperature laboratory where superfluidity can be probed in the atomic scale; they provide an ideal environment for molecular spectroscopy studies and for the synthesis of metastable chemical species.

1.2 Helium-helium interaction

The helium atom has a very stable electronic configuration (the two electrons in the first $1s$-shell) that makes it chemically inert. The interaction between atoms is due to the polarization of the electronic cloud, and the interaction between helium atoms can be considered to be independent of the involved isotopes. The van der Waals interaction when two atoms are close together is rather small and translates into a weak attraction that nevertheless turns into a strong repulsion when the atoms overlap. The interaction depends only on the interparticle distance.

A simple representation of He-He interaction is provided by a Lennard-Jones potential

$$V_{LJ}(r) = 4\epsilon \left[\left(\frac{\sigma}{r}\right)^{12} - \left(\frac{\sigma}{r}\right)^{6} \right], \tag{7}$$

where $\epsilon = 10.22$ K defines the depth of the potential and $\sigma = 2.556$ Å the length scale. Nowadays, more accurate potentials are used in realistic calculations. One of the more popular is the so-called Aziz HFD-B(HE) [13] interaction

$$V_{AZ}(r) = \epsilon \left[A e^{-\alpha x + \beta x^2} - F(x) \left(\frac{C_6}{x^6} + \frac{C_8}{x^8} + \frac{C_{10}}{x^{10}} \right) \right] , \tag{8}$$

where

$$F(x) = \begin{cases} \exp\left[-\left(\frac{D}{x} - 1 \right)^2 \right] & x < D \\ 1 & x \geq D \end{cases} \tag{9}$$

and

$$x = \frac{r}{r_m} \tag{10}$$

The parameter values are

$$\begin{array}{lll} \epsilon = 10.948\,\mathrm{K} & \alpha = 10.43329537 & \beta = -2.27965105 \\ A = 1.8443101 \times 10^5 & r_m = 2.963\,\text{Å} & D = 1.4826 \\ C_6 = 1.36745214 & C_8 = 0.42123807 & C_{10} = 0.17473318 \end{array} \tag{11}$$

The He-He potential is characterized by a strong short range repulsion (such that in a first approximation, the atoms can be considered as hard spheres of diameter $\sim 2.6\,$Å) and a weak attraction at medium and large distances. Lennard-Jones and

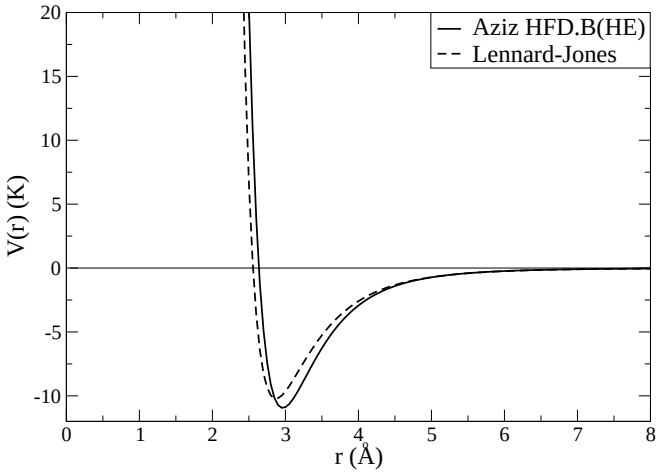

Figure 4: Comparison between the Lennard–Jones and the Aziz HFD-B(HE) [13] Helium-Helium potentials.

Aziz potentials are compared in Fig. 4. Despite the apparent similarities, $V_{AZ}(r)$ appreciably differs from $V_{LJ}(r)$ at short distances where in particular the former does not diverge.

The lowest excitation energy of helium atom is around 20 eV, or about 2.3×10^5 K, in more convenient units. This is quite high a value as compared to the energy scale involved in the description of the liquid, which is of the order of few K. The situation is such that one can safely forget about the internal structure of the atoms and consider them as the elementary constituents of the quantum liquid interacting through a two–body potential. Actually, this interaction is so weak that two ^{4}He atoms are barely bound; the ^{4}He-^{4}He distance in the dimer is 52 ± 4 Å, and its binding energy 1.1 + 0.3 - 0.2 mK [14], while neither two ^{3}He atoms nor a ^{3}He-^{4}He pair are bound.

1.3 Why helium remains liquid down to absolute zero temperature

It is commonly said that any substance solidifies at low enough temperatures. Indeed, cooling down a substance reduces the average kinetic energy of its atoms: at low enough temperatures the atoms lose their mobility and the attractive interaction confines them to fixed positions, so that the substance solidifies. However, in this qualitative argument one is forgetting quantum effects. The uncertainty principle

tells us that if the atoms are confined into a small region in space their momentum cannot be equal to zero, and so they acquire a non–zero average kinetic energy, the so called *zero-point motion*. One way to estimate this energy is to associate the volume occupied by each particle, roughly $1/\rho$, to a spherical box of radius R, and to approximate the kinetic energy to the ground state energy of a particle moving in this spherical box by $E \sim \hbar^2\pi^2/(2mR^2)$. At the saturation density of liquid ^{4}He one atom occupies a volume of 46 Å^3 (the radius is $R = 2.22$ Å), and therefore we estimate the zero-point motion energy $E \sim 12\,\mathrm{K}$. This kinetic energy is large enough to compensate the interaction between the atoms that tries to locate them in fixed equilibrium positions, and that is the reason why helium remains liquid at $T = 0$. The other inert (closed-shell) gases are heavier and easier to polarize, and become solid at zero temperature. Hydrogen is lighter than helium (so that the zero-pont energy is larger) but it is more easily polarizable than helium and the interaction is stronger. Hydrogen become solid at low temperatures, although its boiling point is at $T \simeq 20$ K.

1.4 The superfluidity of liquid helium

Superfluidity means absence of viscosity: a superfluid flows through a capillary with no pressure dropping along the tube. This macroscopic property can be qualitatively understood at a microscopic level, by linking the energy exchanges (between helium and capillary) with the possible excitations of the liquid. Landau derived a simple criterion of superfluidity, based on general arguments of energy and momentum conservation and Galilean invariance. We recall the basic results concerning energy and momentum transformations. Let $\mathbf{p}$ and E be the momentum and energy in a given reference frame of an object of mass M. In a reference frame which moves with velocity $\mathbf{v}$ relative to the former, the momentum and energy are written as $\mathbf{p} - M\mathbf{v}$ and $E - \mathbf{p}\cdot\mathbf{v} + Mv^2/2$, respectively.

Keeping in mind these transformations, let us consider two reference systems. In the laboratory frame, the capillary is at rest and the liquid moves with velocity $\mathbf{v}$. In the liquid frame, the liquid is at rest and the capillary moves with velocity -$\mathbf{v}$. In Table 2 are displayed the expressions of total momentum and energy of the liquid in these frames, assuming no or one excitation in the liquid.

The existence of viscosity produces a change of motion of the liquid, which starts by a gradual occurrence of the internal excitations in the liquid. If an elementary excitation with momentum $\hbar\mathbf{k}$ and energy $\varepsilon(\mathbf{k})$ appears in the liquid, the momentum and energy of the liquid are shifted as indicated in the Table. Therefore in the laboratory frame, the change in energy of the liquid due to the appearance of an elementary excitation is $\varepsilon(\mathbf{k}) + \hbar\mathbf{k}\cdot\mathbf{v}$. Dissipation corresponds to a loss of energy from the fluid to the capillary. An elementary excitation allows dissipation if the energy change in the laboratory frame is negative.

Table 2: Momentum and energy of the liquid in two reference frames.

		Momentum	Energy
Liquid frame	No excitations	0	E_0
	One excitation	$\hbar\mathbf{k}$	$E_0 + \varepsilon(\mathbf{k})$
Lab frame	No excitations	$M\mathbf{v}$	$E_0 + 1/2Mv^2$
	One excitation	$\hbar\mathbf{k} + M\mathbf{v}$	$E_0 + 1/2Mv^2 + \varepsilon(k) + \hbar\mathbf{k}\cdot\mathbf{v}$

The scalar product $\hbar\mathbf{k}\cdot\mathbf{v} = \hbar kv\cos\theta$ has a minimum value attained when $\mathbf{k}$ and $\mathbf{v}$ are collinear and in opposite directions (relative angle $\theta = \pi$). We further assume rotational invariance and thus simply write $\varepsilon(\mathbf{k}) = \varepsilon(k)$ in the following. A necessary condition for dissipation is provided by $\varepsilon(k) - \hbar k\, v < 0$. This defines a critical velocity as the minimum with respect to k of the excitation energy/momentum ratio

$$v_c = \mathrm{Min}_k \, \frac{\varepsilon(k)}{\hbar k} \tag{12}$$

If the liquid moves with a velocity $v > v_c$ relative to the capillary, it is energetically favorable to produce an excitation, then the flow of the liquid is unstable and the kinetic energy is transformed into heat. On the contrary, if the relative velocity is $v < v_c$, no excitation is possible and the liquid flows without dissipation. It is interesting to apply this criterion to a gas of bosons (no interaction between constituents). The elementary excitations are those of single particles, with energy $\varepsilon(k) = \hbar^2k^2/2m$. The critical velocity v_c from Eq. (12) is zero, so that at any value of the relative velocity, the gas always exchanges energy and momentum with the capillary, hence dissipates energy.

The elementary excitation energy $\varepsilon(k)$ as a function of momentum $\hbar k$ is known as the dispersion relation. Landau suggested that there are two kinds of elementary excitations in Helium. In the region of low k, they correspond to the ordinary acoustic waves in a liquid and the dispersion relation is linear $\varepsilon(k) = \hbar kc$, with the slope $c = 238$ m/s being the speed of ordinary sound (or "first sound" in the liquid helium context). Landau called "phonons" these excitations since they are the analogous to longitudinal phonons in a solid, as for example vibrations along the length of a bar. At higher values of k, the pattern of $\varepsilon(k)$ deviates from linear. Its precise form depends on the details of the interaction and it is not an easy task to obtain its general form. Based on general thermodynamical properties, in particular the measure of the specific heat, Landau figured out the existence of another type of excitation, which he called "rotons" assuming for them a parabolic dispersion relation $\varepsilon(k) = \Delta + \hbar^2(k-k_0)^2/2\mu$ around a certain momentum $\hbar k_0$. The parameters (Δ, k_0, μ) are fitted to experimental results. This delivers a phonon-roton dispersion relation which qualitatively agrees with the experimental determination of excitations in He-II, currently measured by neutron scattering, and displayed in

Fig. 5.

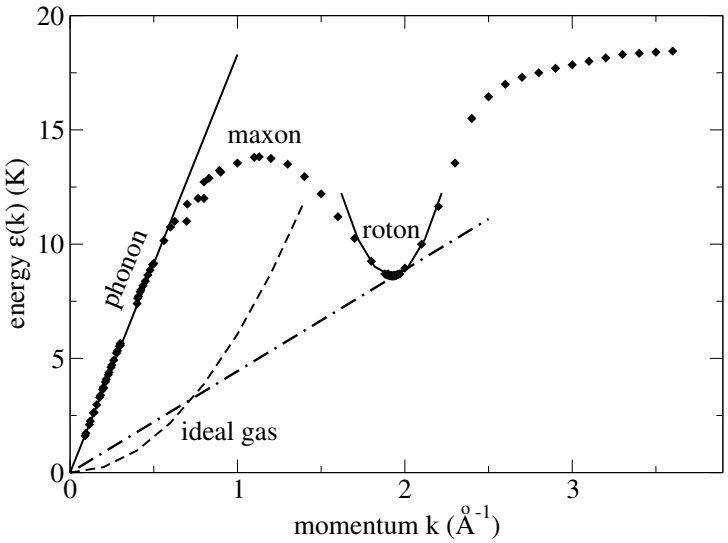

Figure 5: Dispersion relation of liquid ^{4}He, as a function of momentum k. Diamonds: experimental points from Ref. [11]

We note that the phonon-roton dispersion relation is very different from the quadratic k^2-behavior of a non-interacting gas (dashed curve in the figure). Indeed, it starts with a linear part at low wave vectors, $k \leq 0.8$ A^{-1}, which is the phonon region. It is followed by a maximum at $\simeq 1$ A^{-1}, called the maxon region, and then by a pronounced minimum (the roton region) at $\simeq 2$ A^{-1}. There is a final steady rise at large k. Measurements of thermal properties below $\simeq 0.6$ K (as the low-T behavior of the specific heat) suggest that phonons are the only excitation modes. Rotons need a minimum energy (denoted by Δ in the previous reasoning) to be excited, and thus they require higher values of T and/or k.

Let us come back to the critical velocity given in Eq. (12). To determine this velocity, we consider a straight line passing by the origin and tangent to the curve $\varepsilon(k)$. We identify v_c with the minimal slope of this line. From Fig. 5, one can deduce that in the phonon region v_c is equal to the speed of sound $c = 238$ m/s, and the liquid can flow without viscosity for subsonic velocities $v \leq c_1$. In the roton region, the minimum slope fixes a smaller value of the critical velocity $\simeq 58$ m/s. However, the actual critical velocity is much smaller than this value because other modes of excitation, such as vortices, can also be produced. Anyhow, the message from Landau's criterion is that below a certain gap in the excitation energ the system is superfluid. A DFT account of vortices in liquid ^{4}He and droplets can be found in Refs. [1, 2]; see also Ref. [15] for a general description.

The dispersion relation was first microscopically explained by Feynman in terms of the atom-atom interaction and a wave function completely symmetric with respect

to the exchange of any pair of bosons. As a result, Landau's phenomenological guess was qualitatively explained in microscopic terms, by solving the Schrödinger equation. We will come back to this point at the end of Sect. 2.1.

An important question was raised at the end of 1950's by Becker: is superfluidity restricted to bulk liquid? or could it be possible to observe superfluid effects in finite systems, consisting of a small number of helium atoms? Prior to answer the last question it was necessary to produce helium droplets in a controlled way, and this took a long time. Eventually, the group of Toennies in Göttingen demonstrated that small helium droplets do indeed manifest superfluidity. The experiment consisted in observing the rotational spectrum of a single carbonyl sulfide (OCS) molecule embedded into a helium droplet, varying the size of the droplet and comparing the observed spectrum to that of the free OCS molecule. For droplets containing about 60 atoms and more, the OCS molecule rotates freely, with no energy dissipation. See Refs. [16] for the original experiment and interpretation, and [17] for a broad readership presentation.

2 Density Functional Theory and strongly interacting systems

2.1 Microscopic many-body theories and DFT

In a wide sense, we can say that at the most fundamental level nearly all physics is many-body physics. The energy and length scales appropriate to describe a particular physical system define both its microscopic constituents and their interaction, which allows one to deduce the relevant properties of the system. All information we can obtain about the system is contained in its wave function. The main methods or techniques to solve the many-body Schrödinger equation can be roughly grouped in the following categories:

• Perturbative techniques, which are essentially based on expansions in powers of the interaction coupling constant, as Time-Dependent Perturbation Theory and Green's Function or Propagator Methods.
• Expansion of the wave function on a complete basis, as the Configuration Interaction Method and the Coupled Cluster Method.
• Variational techniques, as the Hypernetted Chain Expansion and the Correlated Basis Function method.
• Quantum Monte Carlo methods, which appear in several varieties as Green's function MC, Diffusion MC, Path Integral MC...

The microscopic methods of choice to study liquid ^{4}He are Quantum MC, either DMC at $T = 0$ or PIMC at $T \neq 0$. They give stochastic estimates of the expectation values of some operators, providing for them "exact" results within controlled

statistical errors.

In general, these microscopic methods demand an important computational effort, and for large and complex systems it is nearly impossible to apply them efficiently. A simplest alternative consists in using approximations based on effective interactions, as the mean-field approximation. In all cases, the purpose is to solve the Schrödinger equation and determine the wave function, which contains all the information we can obtain about the system.

However, we do not always need such a complete information. Very often, the information we require to describe a system is contained in the ground state one- and two-body density matrices, defined as

$$\rho_1(\mathbf{r}_1, \mathbf{r'}_1) = N \int \mathrm{d}\mathbf{r}_2 \ldots \mathrm{d}\mathbf{r}_N \Psi^*(\mathbf{r}_1, \mathbf{r}_2, \ldots, \mathbf{r}_N)\Psi(\mathbf{r'}_1, \mathbf{r}_2, \ldots, \mathbf{r}_N) \tag{13}$$

and

$$\rho_2(\mathbf{r}_1, \mathbf{r}_2; \mathbf{r'}_1, \mathbf{r'}_2) = N(N-1) \int \mathrm{d}\mathbf{r}_3 \ldots \mathrm{d}\mathbf{r}_N \Psi^*(\mathbf{r}_1, \mathbf{r}_2, \mathbf{r}_3, \ldots, \mathbf{r}_N)\Psi(\mathbf{r'}_1, \mathbf{r'}_2, \mathbf{r}_3, \ldots, \mathbf{r}_N) \tag{14}$$

The wave function is assumed to be normalized to unity. These density matrices allow us to obtain the ground state expectation value of one- and two-body operators. For instance, the ground state energy $E = \langle\Psi|H|\Psi\rangle$ can be formally written as

$$E = \frac{\hbar^2}{2m} \int \mathrm{d}\mathbf{r} |\nabla \cdot \nabla' \rho_1(\mathbf{r}, \mathbf{r}')|_{\mathbf{r}'=\mathbf{r}} + \frac{1}{2} \int \mathrm{d}\mathbf{r}\mathrm{d}\mathbf{r}' \rho_2(\mathbf{r}, \mathbf{r}'; \mathbf{r}, \mathbf{r}') V(\mathbf{r} - \mathbf{r}') \tag{15}$$

Therefore, if only the value of the ground state energy is sought, only two functions depending on 6 spatial coordinates each are required, instead of the information contained in Ψ, which depends on 3N spatial coordinates. Obviously, the obtention of these two functions is not a simple task, as it contains all the intrincacies related to a many-body system.

Notice that the diagonal one-body density is simply the particle density $\rho_1(\mathbf{r}, \mathbf{r}) = \rho(\mathbf{r})$. It is convenient to define the so-called kinetic energy density

$$\tau(\mathbf{r}) = |\nabla \cdot \nabla' \rho_1(\mathbf{r}, \mathbf{r}')|_{\mathbf{r}'=\mathbf{r}} \tag{16}$$

and the pair-correlation function $g(\mathbf{r}, \mathbf{r}')$ from the diagonal two-body density as

$$\rho_2(\mathbf{r}, \mathbf{r}'; \mathbf{r}, \mathbf{r}') = g(\mathbf{r}, \mathbf{r}')\, \rho(\mathbf{r})\, \rho(\mathbf{r}') \tag{17}$$

The ground state energy reads

$$E = \frac{\hbar^2}{2m} \int \mathrm{d}\mathbf{r}\, \tau(\mathbf{r}) + \frac{1}{2} \int \mathrm{d}\mathbf{r}\mathrm{d}\mathbf{r}' g(\mathbf{r}, \mathbf{r}')\, V(\mathbf{r} - \mathbf{r}')\, \rho(\mathbf{r})\, \rho(\mathbf{r}') \tag{18}$$

Had not be the function g present in the last term, it would be identical to the classical expression of the potential energy. The pair-correlation function indicates the deviation of the system from a "classical" behavior.

2.2 The Hohenberg-Kohn theorem

Hohenberg and Kohn [8] went a step further: the previous description in terms of ρ_1 and ρ_2 still contains too much information. Indeed, they proved that the ground state properties of a quantum system of interacting particles can be characterized solely in terms of the number density $\rho(\mathbf{r})$. In particular, the ground state energy of the system is a unique functional of the density $E[\rho]$. This assertion, which is far from obvious, is the starting point of the Density Functional Theory (DFT). In a general discussion on DFT, one should address rigorous aspects, such as existence theorems or questions related to the possibility of systematically constructing a DFT. Apart from the following general considerations, these issues are not addressed in these lectures.

In their original work, Hohenberg and Kohn [8] assumed a many-body system subject to an external one-body potential $U_e = \sum_i U(\mathbf{r}_i)$. The two-body interaction V characterizes the elementary constituents of the system, and the external potential U_e distinguishes its different physical realisations. For instance, for electronic systems V is the Coulomb interaction between electrons, and U_e distinguishes between their different realizations such as atoms, molecules, solids, etc. (keep in mind that no electronic system can exist without that external potential). The ground state wave function Ψ is the solution of the Schrödinger equation

$$(H + U_e)\Psi = E\Psi \tag{19}$$

For simplicity, we shall assume a central two-body interaction, and a non-degenerate ground state.

Clearly, Ψ is a functional of the external potential, and so is the density $\rho(\mathbf{r})$. We have thus the chain:

$$U_e \Longrightarrow \Psi \Longrightarrow \rho \tag{20}$$

Hohenberg and Kohn showed that these implicational arrows can be reversed

$$U_e \Longleftrightarrow \Psi \Longleftrightarrow \rho \tag{21}$$

so that there is a one-to-one correspondence between these three quantities. In particular, Eq. (21) means that the functions Ψ and ρ contains the same information. Choosing ρ as the main function it results that the ground state wave function Ψ of the system is a unique functional of the ground state one-body density ρ. The external potential U_e is also a unique functional of the ground state density. However, this equivalence raises some unicity questions (the so-called v-representability) which we are not going to discuss here (see Ref. [10]).

As a corollary, the ground state expectation value of any observable represented by an operator Q is a unique functional of the one-body density:

$$\langle \Psi[\rho]|Q|\Psi[\rho]\rangle = Q[\rho] \tag{22}$$

If Q is the Hamiltonian, one deduces that the ground state energy is a unique functional of the density. It can be written as

$$E[\rho] = T[\rho] + V[\rho] + \int \mathrm{d}\mathbf{r}\rho(\mathbf{r})U_e(\mathbf{r}) \tag{23}$$

where

$$T[\rho] = \langle\Psi|T|\Psi\rangle \tag{24}$$

and

$$V[\rho] = \langle\Psi|V|\Psi\rangle \tag{25}$$

are the kinetic and potential energy functionals, respectively. They are universal functionals, in the sense that they are the same for any electronic system, either atoms, molecules or solids, irrespective of the specific external potential and number of particles.

The functional $E[\rho]$ can be defined for any density, but for the ground state density one obtains the minimum energy value. The variational principle insures that when the expectation value of the total Hamiltonian

$$\langle\Psi|T + V + U_e|\Psi\rangle \tag{26}$$

is calculated varying Ψ (and keeping constant the number of particles), it has a minimum at the true ground state wave function Ψ. Translating this in terms of the density, it results that the exact ground state density can be determined by minimizing the functional $E[\rho]$ with respect to ρ, restricted to a fixed number of particles, i.e.

$$\delta\left\{E[\rho] - \mu\int \mathrm{d}\mathbf{r}\rho(\mathbf{r})\right\} = 0 \tag{27}$$

where μ is a Lagrange multiplier. This is the chemical potential, which insures the conservation of the particle number. Once determined the minimum, any ground state property, represented by a generic operator Q, can be calculated. We have simply to plug the ground state density in the corresponding functional $Q[\rho]$.

Up to now, everything is exact but not very useful for practical purposes. The Hohenberg-Kohn theorem proves the existence and unicity of the ground state energy functional, but give no clue about its explicit form. The main task in DFT is to construct good approximations to $E[\rho]$ and the functionals for the operators relevant for the properties of the system we want to study. The explicit form of the functional $E[\rho]$ has to be constructed through a wise mixture of exact and approximated terms. DFT is not a precision method which, in principle, can be pushed systematically to arbitrary accuracy. It contains an important phenomenological component, whose final justification is the quality of its predictions. But DFT is the real alternative to the above mentioned microscopic methods for systems consisting of many constituents, and also for smaller systems when moderate accuracy is sufficient.

The previous arguments seem to be quite general, as we have only used the Schrödinger equation (hence the specific interaction) and the variational principle. Therefore, these results are valid for any system of fermions, bosons or mixed fermions and bosons. However, we must take into account the symmetry properties of the wave function, even if they were not explicit in the proof of Hohenberg-Kohn theorem. Take for instance a non-interacting system of helium atoms. The Hohenberg-Kohn theorem establishes the existence and unicity of the kinetic energy functional, and one can convince oneself that the functional is different for bosons and fermions, because of the different statistics. (We will address this issue in 2.4.) Hence, although the interaction between helium atoms is the same for both isotopes, the density functional is isotopic dependent, and its explicit construction must be supplemented by the specification of the statistical character of the constituents of the system.

2.3 Functional calculus in a nutshell

Loosely speaking, a function $y = f(x)$ is a rule for going from a number x to a number y or, more generally, a function maps from a finite-dimensional vector to a single number. For instance, the density function ρ maps from the space vector $\mathbf{r}$ to the number $\rho(\mathbf{r})$; the wave function $\Psi(\mathbf{r}_1, \ldots, \mathbf{r}_N)$ maps from the set $\{\mathbf{r}_i\}$ of N vectors to the (complex) number Ψ. By contrast, a functional maps from a function to a number. The total number of particles N is an example of a functional of the density $\rho(\mathbf{r})$, given by $N = \int d\mathbf{r}\rho(\mathbf{r})$. In general, a functional may depend on the function and also its derivatives.

As a practical example, let us consider the energy E of a many-body system as a functional of the density ρ, written as

$$E[\rho] = \int d\mathbf{r}\, \mathcal{E}[\rho(\mathbf{r}), \nabla\rho(\mathbf{r}), \Delta\rho(\mathbf{r})] \tag{28}$$

where $\mathcal{E}$ is the energy density (i.e. the energy per unit of volume), which for the sake of simplicity is assumed to contain at most second order derivatives of the density. Let us calculate the first-order change of $E[\rho]$ due to an arbitrary change in the function ρ. In general, one could impose some constraints, as for instance keeping constant the expectation values of specific operators, which is done by introducing Lagrange parameters. We consider here the variation keeping fixed the number of particles N, with the chemical potential μ as Lagrange multiplier. The variation we are looking for is

$$\delta\left\{E[\rho] - \mu\int d\mathbf{r}\rho(\mathbf{r})\right\} = 0 \tag{29}$$

When the density ρ is changed to $\rho + \delta\rho$ his equation writes

$$\int d\mathbf{r}\,\{\mathcal{E}[\rho + \delta\rho, \nabla(\rho + \delta\rho), \Delta(\rho + \delta\rho)] - \mathcal{E}[\rho, \nabla\rho, \Delta\rho] - \mu\delta\rho\} \tag{30}$$

Expanding the first term up to first order in $\delta\rho$:

$$\int d\mathbf{r} \left\{ \frac{\partial \mathcal{E}}{\partial \rho}\delta\rho + \frac{\partial \mathcal{E}}{\partial \nabla\rho}\nabla\delta\rho + \frac{\partial \mathcal{E}}{\partial \Delta\rho}\Delta\delta\rho - \mu\delta\rho \right\} = 0 \tag{31}$$

and integrating by parts the 2nd and 3rd terms

$$\int d\mathbf{r} \left\{ \frac{\partial \mathcal{E}}{\partial \rho} - \nabla\frac{\partial \mathcal{E}}{\partial \nabla\rho} + \Delta\frac{\partial \mathcal{E}}{\partial \Delta\rho} - \mu \right\} \delta\rho = 0 \tag{32}$$

As this equation should be satisfied for an arbitrary variation $\delta\rho$, we are left with

$$\frac{\partial \mathcal{E}}{\partial \rho} - \nabla\frac{\partial \mathcal{E}}{\partial \nabla\rho} + \Delta\frac{\partial \mathcal{E}}{\partial \Delta\rho} = \mu \tag{33}$$

which is the Euler-Lagrange equation for our extremal problem. In general, this is an integro-differential equation, which has to be solved with the appropriate boundary conditions, see e.g. Ref. [3].

2.4 The Kohn-Sham scheme

The Hohenberg Kohn variational principle can be recast in the form of exact single-particle self-consistent equations, similar to the Hartree equation, which are called Kohn-Sham equations [9]. In the case of electronic systems it is customary to write the energy functional as

$$E[\rho] = T_s[\rho] + \int \mathrm{d}\mathbf{r}\rho(\mathbf{r})U_e(\mathbf{r}) + \frac{1}{2}\int\int \mathrm{d}\mathbf{r}\mathrm{d}\mathbf{r}' V(\mathbf{r}-\mathbf{r}')\rho(\mathbf{r})\rho(\mathbf{r}') + E_{xc}[\rho] \tag{34}$$

where $T_s[\rho]$ is the kinetic energy functional of the non-interacting system (the subindex s means single-particle) with density ρ, and $E_{xc}[\rho]$ is the so-called exchange-correlation term. It is formally defined as

$$E_{xc}[\rho] = T[\rho] - T_s[\rho] + V[\rho] - \frac{1}{2}\int\int \mathrm{d}\mathbf{r}\mathrm{d}\mathbf{r}' V(\mathbf{r}-\mathbf{r}')\rho(\mathbf{r})\rho(\mathbf{r}') \tag{35}$$

We have simply added and subtracted two terms: i) the kinetic energy functional of the non-interacting system (yet unknown), and ii) the classical expression of the potential energy of an interacting system with density ρ. All the complexities (and our ignorance) of the many-body problem are contained in E_{xc}, which is in general a very complicated object. Had we wished its exact expression we should use our favorite microscopic many-body method. The interesting point with DFT is that it is possible to obtain relatively simple approximations for E_{xc}, leading to reasonably accurate results. Before considering such approximations, we shall establish a practical scheme for the calculation.

Let us apply the variational principle to the ground state energy functional i.e.

$$\delta \left\{ E[\rho] - \mu \int d\mathbf{r} \rho(\mathbf{r}) \right\} = 0 \tag{36}$$

whose meaning is that the functional is stationary for small variations $\delta\rho$ of the density around the ground state density ρ_0. Using expression (34), this equation can be more explicitely written as

$$\delta T_s[\rho] + \int d\mathbf{r}\, \delta\rho(\mathbf{r}) \left[U_e(\mathbf{r}) + \int d\mathbf{r}' V(\mathbf{r}-\mathbf{r}')\rho(\mathbf{r}') + V_{xc}[\rho] - \mu \right] = 0 \tag{37}$$

where

$$V_{xc}[\rho] = \frac{\delta \mathcal{E}_{xc}[\rho]}{\delta\rho} \tag{38}$$

is the so-called exchange-correlation potential, where $\mathcal{E}_{xc}$ is the exchange-correlation energy density, $E_{xc}[\rho] = \int d\mathbf{r}\, \mathcal{E}_{xc}(\rho)$.

Minimizing the energy functional $E[\rho]$ is equivalent to solving a single-particle problem, corresponding to the one-body Hamiltonian $T_s + \sum_i U_s(\mathbf{r}_i)$, with the identification

$$U_s(\mathbf{r}) = U_e(\mathbf{r}) + \int d\mathbf{r}' V(\mathbf{r}-\mathbf{r}')\rho(\mathbf{r}') + V_{xc}[\rho] \tag{39}$$

The exact solution of this problem can be obtained in terms of a set of single-particle states $\{\phi_i\}$. The ground state energy is minimized with respect to the single-particle orbitals (this is equivalent to minimize it with respect to the density), and one gets

$$\left[-\frac{\hbar^2}{2m}\nabla^2 + U_s(\mathbf{r}) \right] \phi_i = \epsilon_i \phi_i \tag{40}$$

where ϵ_i are Lagrange multipliers, insuring the normalization of ϕ_i.

The problem has been translated to an equivalent Hartree problem, with particles subject to an external potential. At this level, the single-particle orbitals and energies are simply mathematical tools to calculate the real physical quantities, namely the ground state density and energy. The former is written as

$$\rho(\mathbf{r}) = \sum_i |\phi_i|^2 \tag{41}$$

To compute the latter we use the expression

$$\sum_i \epsilon_i = \sum_i \langle \phi_i | -\frac{\hbar^2}{2m}\nabla^2 + U_s(\mathbf{r}) | \phi_i \rangle = T_s[\rho] + \int d\mathbf{r} U_s(\mathbf{r})\rho(\mathbf{r}) \tag{42}$$

to eliminate the functional $T_s[\rho]$ in $E[\rho]$. The ground state energy can thus be written as

$$E = \sum_i \epsilon_i - \frac{1}{2}\int\int \mathrm{d}\mathbf{r}\mathrm{d}\mathbf{r}' V(\mathbf{r}-\mathbf{r}')\rho(\mathbf{r})\rho(\mathbf{r}') + E_{xc}[\rho] - \int \mathrm{d}\mathbf{r} V_{xc}[\rho]\rho(\mathbf{r}) \tag{43}$$

The Kohn-Sham Eq. (40) has to be solved consistently, because the external potential depends on the density ρ which in turn depends on the solutions ϕ_i of the equation.

Let's come back to the dependence of the kinetic energy density functional on quantum statistics. Consider the ground state of a system of particles described by single-particle orbitals. We know that In the case of bosons all of them occupy the same quantum state, defined by a single orbital $\phi_0(\mathbf{r})$ which characterizes the condensate. The particle density is written as $\rho(\mathbf{r}) = N|\phi_0(\mathbf{r})|^2$. The kinetic energy functional is

$$T_s[\rho] = -\frac{\hbar^2}{2m}\int \mathrm{d}\mathbf{r}\, N\, \phi_0^*(\mathbf{r})\Delta\phi_0(\mathbf{r}) = \frac{\hbar^2}{2m}\int \mathrm{d}\mathbf{r}\, N\, |\nabla\phi_0(\mathbf{r})|^2 \tag{44}$$

As there is a single orbital, the kinetic energy density $\tau_s(\mathbf{r}) = N|\nabla\phi_0(\mathbf{r})|^2$ can be cast into the equivalent forms

$$\tau_s(\mathbf{r}) = \frac{\left(\nabla\rho(\mathbf{r})\right)^2}{4\rho(\mathbf{r})} \equiv \left(\nabla\sqrt{\rho(\mathbf{r})}\right)^2 \tag{45}$$

This is the *exact* density functional for the ground state of bosons.

In the case of fermions we deal with the kinetic energy density

$$\tau_s(\mathbf{r}) = \sum_i |\nabla\phi_i(\mathbf{r})|^2$$

where the sum runs over all occupied single-particle states. An exact density functional is obtained only for an infinite and homogeneous system of fermions. Otherwise, it is preferable to follow the Kohn-Sham scheme and use the orbitals as an intermediate step between the kinetic energy and the particle densities.

2.5 Systems with strong repulsion at short distances

DFT was originally used for electronic systems, starting from the following density functional energy of a many-body system

$$E[\rho] = T_s[\rho] + \int d\mathbf{r} U_e(\mathbf{r})\rho(\mathbf{r}) + \frac{1}{2}\int\int \mathrm{d}\mathbf{r}\mathrm{d}\mathbf{r}' V(\mathbf{r}-\mathbf{r}')\rho(\mathbf{r})\rho(\mathbf{r}') + E_{xc}[\rho] \tag{46}$$

where $V(r) = e^2/r$ is the Coulomb interaction between electrons. The third term in the above equation has precisely the classical expression, which neglects any exchange between quantal particles. Exchange and correlation effects are included in the last term E_{xc}. In most cases, neglecting it is not too bad an approximation, which is improved by using physical intuition and phenomenology to construct approximations for E_{xc}.

However, for liquid helium we are in trouble if we use this functional as a starting point, because the interaction V is characterized by a strong repulsion at short distances. The Lennard-Jones interaction is strictly infinity at the origin (recall the term $1/r^{12}$), and the more appropriate HFD-B(HE) Aziz interaction has a repulsion of $\simeq 2 \times 10^6$ K at the origin, to be compared with the attraction of $\simeq -10$ K at the bottom of the well. The volume integral of the Aziz interaction is $\simeq 9.30 \times 10^5$ K Å^3, giving a contribution of $\simeq 2.05 \times 10^4$ K to the energy per particle of the homogeneous liquid. This implies that by no means E_{xc} can be taken as a small correction.

Let us come back to the microscopic expression for the energy, as given in Eq. (18), which we write here again

$$E = \frac{\hbar^2}{2m} \int \mathrm{d}\mathbf{r}\, \tau(\mathbf{r}) + \frac{1}{2} \int \int \mathrm{d}\mathbf{r} \mathrm{d}\mathbf{r}'\, g(\mathbf{r}, \mathbf{r}')\, V(\mathbf{r} - \mathbf{r}')\, \rho(\mathbf{r}) \rho(\mathbf{r}') \tag{47}$$

In Fig. 6 is plotted the pair correlation for liquid ^{4}He (notice that in the bulk g depends only on $|\mathbf{r} - \mathbf{r}'|$). One can see that $g(r)$ vanishes at short distances, where the interaction becomes infinite or very large. In other words, in the regions where the interaction becomes very repulsive the pair correlation function is adequately small. It is clear that this role cannot be played by the product $\rho(\mathbf{r})\rho(\mathbf{r}')$ of one-body densities. The short-range repulsion is screened by the pair correlation function.

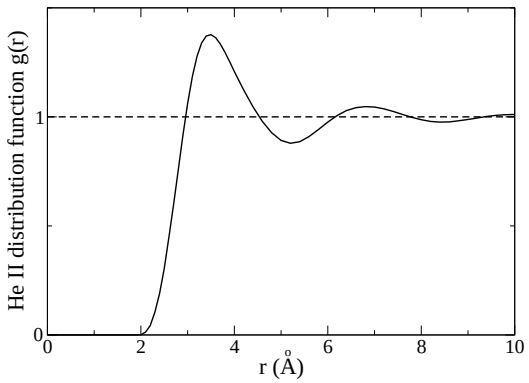

Figure 6: Pair correlation function in superfluid ^{4}He.

To deal with strongly repulsive potentials, there are two possibilities. The first one is to construct a DFT involving both the one-body density and the pair correlation function. Although this generalization of the Hohenberg-Kohn theorem has been sketched, to the best of our knowledge its practical implementation has been limited to a single trial for each helium isotope [31, 32]. The second alternative is to construct a phenomenological density functional, which is precisely the aim of Sect. 3.

The idea is to write down a density functional assuming an effective atom-atom interaction. The starting point is

$$E[\rho] = T_s[\rho] + \int d\mathbf{r} U_e(\mathbf{r})\rho(\mathbf{r}) + \frac{1}{2}\int\int \mathrm{d}\mathbf{r}\mathrm{d}\mathbf{r}' V_{\mathrm{eff}}(\mathbf{r}-\mathbf{r}')\rho(\mathbf{r})\rho(\mathbf{r}') + E_{xc}[\rho] \qquad (48)$$

The exact expression of the exchange-correlation energy is

$$E_{xc}[\rho] = T[\rho] - T_s[\rho] + \frac{1}{2}\int\int \mathrm{d}\mathbf{r}\mathrm{d}\mathbf{r}'\Big\{g(\mathbf{r},\mathbf{r}')\,V(\mathbf{r}-\mathbf{r}') - V_{\mathrm{eff}}(\mathbf{r}-\mathbf{r}')\Big\}\rho(\mathbf{r})\rho(\mathbf{r}') \quad (49)$$

We have to determine an appropriate effective interaction, besides the exchange-correlation term. After guessing some forms for them one eventually writes a functional depending upon a number of free parameters. They are fixed by fitting experimental values of given physical quantities, as the energy per particle, the equation of state, the speed of sound, etc. as functions of the density.

Before closing this subsection, let us made a comment about the external potential. In electronic systems it guarantees the electric neutrality and hence the stability of the system. No electronic system can exists without the term U_e, whose form specifies the particular system under consideration (i.e. atoms, molecules, solids...). By contrast, helium systems (or atomic nuclei) are self-bound systems, with no external potential. This raises some questions regarding the direct translation of the Hohenberg-Kohn theorem to helium systems, where an external potential typically reflects the presence of atomic or molecular impurities. We do not enter into these considerations, and adopt an heuristic view to apply DFT and construct specific functionals to these systems.

2.6 Response function and DFT

Consider a *homogeneous* system of interacting particles subject to an external periodic perturbation described by the operator

$$\hat{V}_e = \hat{\rho}^+_{\mathbf{q}} Q(\mathbf{q},\omega)\mathrm{e}^{-i\omega t} + \hat{\rho}_{\mathbf{q}} Q^+(\mathbf{q},\omega)\mathrm{e}^{i\omega t} \qquad (50)$$

with

$$\hat{\rho}_{\mathbf{q}} = \sum_i \mathrm{e}^{i\mathbf{q}\cdot\mathbf{r}_i} \qquad (51)$$

where $\mathbf{r}_i$ is the position of the i-th particle. The operator $\hat{\rho}_{\mathbf{q}}$ is the Fourier transform of the density operator $\hat{\rho}(\mathbf{r}) = \sum_i \delta(\mathbf{r}-\mathbf{r}_i)$. In an homogeneous system the ground state expectation value of $\hat{\rho}_{\mathbf{q}}$ vanishes for any finite $\mathbf{q}$, and this is why this operator is called the density fluctuation operator. Its values at finite $\mathbf{q}$ give information about the inhomogeneities of the system. For a weak enough external field, the average fluctuation of the density is proportional to the external field

$$\delta\rho(\mathbf{q},t) = \chi(\mathbf{q},\omega)Q(\mathbf{q},\omega)\mathrm{e}^{-i\omega t} \qquad (52)$$

and the function $\chi(\mathbf{q},\omega)$ is the density-density response function of the system. Other responses (as current-current or spin-spin) are analogously defined. See Refs [15, 30] for an introduction to linear response theory that uses similar concepts as those employed here.

The linear response function is calculated at first-order perturbation theory by assuming that the external operator is introduced adiabatically. The general expression is

$$\chi(\mathbf{q},\omega) = \frac{1}{N}\sum_{n\neq 0}\left\{\frac{|\langle n|Q|0\rangle|^2}{\hbar\omega - E_{n0} + i\eta} - \frac{|\langle n|Q|0\rangle|^2}{\hbar\omega + E_{n0} + i\eta}\right\} \tag{53}$$

where η is a positive quantity arbitrarily small, associated with the adiabatic condition on the external field. For practical calculations one uses the identity

$$\lim_{\eta\to 0^+}\frac{1}{x-a+i\eta} = \mathcal{P}\frac{1}{x-a} - i\pi\delta(x-a)\,, \tag{54}$$

where $\mathcal{P}$ stands for principal part. The imaginary part of the response function defines the structure function (also called dynamic form factor or strength function) as

$$S(\mathbf{q},\omega) = -\frac{1}{\pi}\mathrm{Im}\,\chi(\mathbf{q},\omega) \tag{55}$$

This relation is valid at zero temperature. Otherwise, thermal effects include the possibility of excite and de-excite the system, which implies positive and negative values for ω.

The poles of the response function are related to collective excitations of the system. In particular, for liquid helium the energies $\hbar\omega$ as a function of momentum $\hbar q$ gives the dispersion relation whose measured values are plotted in Fig. 5. Very often the properties of the system relevant to experimental measurements can be directly related to the structure function. For instance, the differential cross section neutron scattering off liquid helium is directly proportional to $S(\mathbf{q},\omega)$. In other cases, experimental outputs are related to energy integrals of $S(\mathbf{q},\omega)$ wheighted with some kinematic function.

Eq. (53) can be easily calculated to get the density-density response for a homogeneous system of non-interacting bosons, for which the orbitals are plane-waves $\mathrm{e}^{i\mathbf{k}\cdot\mathbf{r}_i}$. The ground state $|0\rangle$ corresponds to the condensate with $\mathbf{k} = 0$, and the external operator $Q = \rho_{\mathbf{q}}$ determines the possible excited orbitals. It creates a "particle-hole" pair, that is it removes a particle from the ground state (a "hole" with $\mathbf{k} = 0$) and promotes it to the excited state $|n\rangle$ (a "particle" with $\mathbf{k} = \mathbf{q}$). We are left with

$$\chi_0(\mathbf{q},\omega) = \frac{\frac{\hbar^2\mathbf{q}^2}{m}}{\hbar^2(\omega+i\eta)^2 - \left(\frac{\hbar^2\mathbf{q}^2}{2m}\right)^2} \tag{56}$$

and

$$S_0(\mathbf{q},\omega) = \delta\left(\hbar\omega - \frac{\hbar^2\mathbf{q}^2}{2m}\right) \tag{57}$$

In general, the exact linear density response of the interacting homogeneous system can be written as

$$\chi(\mathbf{q},\omega) = \frac{\chi_0(\mathbf{q},\omega)}{1 - V_{ph}(\mathbf{q})\chi_0(\mathbf{q},\omega)} \tag{58}$$

where $V_{ph}(\mathbf{q})$ is the interaction in $\mathbf{q}$-space between the particle and the hole created by the excitation operator. The particle-hole interaction is the relevant quantity to calculate the response function and related quantities. Within a DFT scheme, it is given by the second functional derivative of the energy:

$$V_{ph}(\mathbf{r},\mathbf{r}') = \frac{\delta^2 E[\rho]}{\delta\rho(\mathbf{r})\delta\rho(\mathbf{r}')} = V_{\text{eff}}(\mathbf{r}-\mathbf{r}') + \frac{\delta^2 E_{xc}[\rho]}{\delta\rho(\mathbf{r})\delta\rho(\mathbf{r}')} \tag{59}$$

In momentum-space:

$$V_{ph}(\mathbf{q}) = \frac{\rho}{\Omega}\int\int d\mathbf{r}d\mathbf{r}'\, \mathrm{e}^{i\mathbf{q}\cdot(\mathbf{r}-\mathbf{r}')}\, V_{ph}(\mathbf{r},\mathbf{r}') \tag{60}$$

In solids and liquids, the correlation function $g(r)$ is experimentally deduced from neutron scattering or X-ray diffraction. An incident beam, characterized by a given value of the momentum, is scattered by the constituents of the target system. The intensity of the deflected beam is analyzed in terms of its momentum and deflecting angle. Let us denote by $\hbar\mathbf{q}$ the difference between the incident and the scattered momenta. The measured intensity is proportional to the static structure factor $S(\mathbf{q})$, defined as the following expectation value:

$$S(\mathbf{q}) = \frac{1}{N}\left\langle\left|\sum_i \exp(\mathrm{i}\mathbf{q}\cdot\mathbf{r}_i)\right|^2\right\rangle = 1 + \frac{1}{N}\left\langle\sum_{i\neq j}\mathrm{e}^{i\mathbf{q}\cdot(\mathbf{r}_i-\mathbf{r}_j)}\right\rangle$$

Actually $S(\mathbf{q})$ is the energy integral of $S(\mathbf{q},\omega)$, or zeroth energy weighted sum rule. Microscopically, the structure factor can further be written as:

$$S(\mathbf{q}) = 1 + \frac{1}{N}\int\int \mathrm{d}\mathbf{r}_1\mathrm{d}\mathbf{r}_2\, \mathrm{e}^{i\mathbf{q}\cdot(\mathbf{r}_1-\mathbf{r}_2)}\, g(\mathbf{r}_1-\mathbf{r}_2)\rho(\mathbf{r}_1)\rho(\mathbf{r}_2)$$

For a homogeneous system, we have:

$$S(\mathbf{q}) = 1 + \varrho\int \mathrm{d}\mathbf{r}\, e^{i\mathbf{q}\cdot\mathbf{r}}\, g(\mathbf{r})$$

The second term above, apart from the ϱ factor, is nothing else than the Fourier transform of $g(\mathbf{r})$. One therefore accesses the pair correlation function from the

structure factor by Fourier transform. This connection between measured structure factor and pair correlation is used in Sec. 1.4, in connection with the superfluidity of liquid helium.

We have mentioned that the dispersion relation of HeII was first microscopically explained by Feynman in terms of a wave function completely symmetric with respect to the exchange of any pair of bosons, and the atom-atom interaction. As a result he obtained a relation between the dispersion relation and the static structure factor $\varepsilon(\mathbf{q}) = \hbar^2\mathbf{q}^2/[2m\,S(\mathbf{q})]$. In Fig. 7 is plotted the structure factor of superfluid helium determined by means of neutron scattering. One can see that $S(\mathbf{q})$ starts by

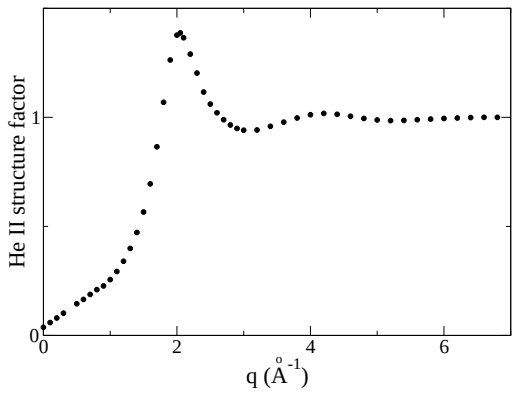

Figure 7: Static structure function measured in superfluid ^{4}He by neutron scattering. Data from Ref. [11]

increasing linearly with q, rises to a maximum at $q_{\max} \simeq 2$ Å^{-1}, and falls afterwards to approach the limit unit, with small amplitude oscillations. Consequently, $\varepsilon(q)$ also starts linearly with q, exhibits a maximum followed by a dip with a minimum and rises again as $\hbar^2q^2/2m$. This is how the phenomenological guess by Landau is qualitatively explained in microscopic terms.

3 DFT for ^{4}He systems

In the density functional approach the ground state of a ^{4}He system *at zero temperature* is described as a Boson condensate: all atoms occupy the lowest energy level, characterized by a single-particle wave function ϕ_0. The particle number density is given by $\rho = N|\phi_0|^2$, and the kinetic energy density is exactly written in terms of ρ as $\tau_s = |\nabla\rho|^2/4\rho = |\nabla\sqrt{\rho}|^2$. Ground state configurations are obtained by minimizing the total energy of the system with respect to the density (Euler-Lagrange equation), or equivalently with respect to the single-particle wave function (KS equation). For

a pure ^{4}He system (no impurity), we start from the density functional

$$E[\rho] = \int d\mathbf{r} \frac{\hbar^2}{2m} \left(\nabla \sqrt{\rho(\mathbf{r})} \right)^2 + \frac{1}{2} \int \int d\mathbf{r}\, d\mathbf{r}'\, V_{\rm eff}(\mathbf{r} - \mathbf{r}') \rho(\mathbf{r}) \rho(\mathbf{r}') + E_{xc}[\rho] \tag{61}$$

and cast the resulting equation in the form

$$\left\{ -\frac{\hbar^2}{2m} \nabla^2 + U_s(\mathbf{r}) \right\} \sqrt{\rho(\mathbf{r})} = \mu \sqrt{\rho(\mathbf{r})} \tag{62}$$

The KS potential writes

$$U_s(\mathbf{r}) = \int d\mathbf{r}'\, V_{\rm eff}(\mathbf{r} - \mathbf{r}') \rho(\mathbf{r}') + V_{xc}[\rho(\mathbf{r})] \tag{63}$$

with $V_{xc} = \delta \mathcal{E}_{xc} / \delta \rho$, assuming that $\mathcal{E}_{xc}$ does not depend on gradients of the density. We shall now consider how to fix the explicit forms of both the effective interaction $V_{\rm eff}$ and the exchange-correlation term E_{xc}.

3.1 Zero-range functionals

In his pioneering work, Stringari [18] adapted a Skyrme-like functional for atomic nuclei [19] to investigate liquid ^{4}He properties. The functional writes

$$E = \int d\mathbf{r} \left\{ \frac{\hbar^2}{2m} \left(\nabla \sqrt{\rho(\mathbf{r})} \right)^2 + \frac{1}{2} b \rho^2 + \frac{1}{2} c \rho^{2+\gamma} + d \left(\nabla \rho \right)^2 \right\} \tag{64}$$

Identifying with Eq. (61) one gets

$$V_{\rm eff}(\mathbf{r}) = b\, \delta(\mathbf{r}) \tag{65}$$

$$E_{xc} = \int d\mathbf{r} \left(\frac{1}{2} c \rho^{2+\gamma} + d \left(\nabla \rho \right)^2 \right) \tag{66}$$

A zero-range effective interaction has been chosen in the form of a delta function. The density-dependence of the exchange-correlation term appears as a power ρ^γ and the squared gradient of ρ. This functional depends on four free parameters b, c, γ, and d. We discuss now how to fix the first three, leaving to Sect. 3.3 the determination of d.

Let us consider the homogeneous liquid ^{4}He, with a constant particle number density. The gradient terms entering Eq. (64) vanish, and the energy per particle is simply given by the integrand, divided by the (constant) density:

$$\frac{E}{N} = \frac{1}{2} b \rho + \frac{1}{2} c \rho^{1+\gamma} \tag{67}$$

It is worth keeping in mind that the fact that $T_s = 0$ in the homogeneous system does not imply that the ground state energy of a boson system is kinetic energy

independent. Actually, by looking to the definition of the exchange-correlation energy given in Eq. (35), we realize that it contains the term $T[\rho] - T_s[\rho]$. The kinetic energy contribution is therefore 'hidden' in the phenomenological parameters c, γ and d of the present functional.

Parameters b, c, γ can be determined by fitting the energy per particle e_0, the density ρ_0 and the speed of sound c_0 (or the compressibility κ_0) at the equilibrium point (see Table 1), whose expressions are:

$$e_0 = \frac{1}{2} b \rho_0 + \frac{1}{2} c \rho_0^{1+\gamma} \tag{68}$$

$$0 = \frac{1}{2} b + \frac{1+\gamma}{2} c \rho_0^{\gamma} \tag{69}$$

$$m c_0^2 = b \rho_0 + \frac{(1+\gamma)(2+\gamma)}{2} c \rho_0^{1+\gamma} \tag{70}$$

The parameters of the so-called ST functional [20] are given in Table 3.

Table 3: Parameters of the ST functional for liquid ^{4}He.

b (K Å^3)	c (K Å$^{3(1+\gamma)}$)	γ	d (K Å^5)
-888.81	1.04554×10^7	2.8	2383

Interestingly, by fitting three quantities at one value of the density, one obtains a fine agreement with experiment in a large interval of density values, as shown in Fig. 2. There is also agreement with microscopic calculations, such as diffusion Monte Carlo in the region not yet accessible by experiments, from saturation down to the spinodal point. The spinodal line is defined by the points at which the speed of sound vanishes; it is a function of T and ρ.

From Eq. (67) we see that in bulk ^{4}He the equilibrium energy per particle ϵ_0 (-7.15 K) is obtained as the sum of -9.70 K (b-term) and +2.55 (c-term). The term proportional to b corresponds to an effective attraction, the one proportional to c to a density-dependent repulsion. Each of them has a different power of ρ. As one could expect, the higher the density the higher the correlation effects.

The previous choice for the density functional is not unique, of course. Actually, it suffices to fit three quantities at the saturation density, namely the energy per particle, the pressure and the speed of sound, to achieve a good agreement with experiment beyond the saturation point. For instance, one can try an expression containing integer powers of the density as

$$E/N = \frac{1}{2} b \rho + \frac{1}{2} c_2 \rho^2 + \frac{1}{3} c_3 \rho^3 \tag{71}$$

By fixing the parameters as in the ST case one obtains the values $b = -718.99$ KÅ^3, $c_2 = -2.411857 \times 10^4$ KÅ^6, $c_3 = 1.858496 \times 10^6$ KÅ^9.

A word about correlations. Within a microscopic description, dynamical correlations are explicitly taken into account when constructing the many-body wave function. In contrast, within the DF approach correlations are implicitly considered in the fit of the parameters to experimental quantities. As a consequence, correlation effects show up in an indirect fashion, or implicitly in quantities such as the energy per particle or the density profiles. From this perspective, it is meaningless to strive for a microscopic description of the correlations within DFT.

3.2 Finite-range functionals

It is quite obvious that the previous zero-range DF misses one important property of the atom-atom interaction, namely the asymptotic r^{-6} behavior characteristic of van der Waals potentials. A way to include this effect into the ST functional for ^{4}He was suggested in Ref. [22].

An obvious improvement over ST is to take as effective interaction a Lennard-Jones potential but screened at short distances

$$\begin{aligned} V_{\rm eff}(r) &= 4\varepsilon\left[\left(\frac{\sigma}{r}\right)^{12} - \left(\frac{\sigma}{r}\right)^{6}\right] \qquad r \geq h \\ &= V_{\rm in}(r) \qquad\qquad\qquad\qquad \text{otherwise} \end{aligned} \tag{72}$$

There exist in the literature several choices regarding the effective range h and the form of the softened potential $V_{\rm in}(r)$ at short distances. We consider here three of them, named as OP (Orsay-Paris) [22], BB (Barcelona-Buenos Aires) [23] and OT (Orsay-Trento) [24].

$$V_{\rm in}^{OP}(r) = V_{LJ}(h)\left(\frac{r}{h}\right)^4 \tag{73}$$

$$V_{\rm in}^{BB}(r) = V_0\left[1 - \left(\frac{r}{\sigma}\right)^8\right] \quad , \quad h = \sigma \tag{74}$$

$$V_{\rm in}^{OT}(r) = 0 \tag{75}$$

The OP choice is a short-range part going smoothly to zero as r^4, the BB choice was inspired by the theory of polarization potentials theory by Pines and collaborators [25], the OT choice is more radical: the inner part is put to zero. To guarantee that the finite range DF does not disrupt the description of the bulk properties of the zero-range DF, one can view the parameter b of the ST interaction (see Eq. 65) other way round, as the volume integral of the effective interaction $b = \int {\rm d}\mathbf{r} V_{\rm eff}(r)$. Imposing this condition over the volume integral of $V_{\rm eff}(r)$, one fixes either V_0 or h.

$$OP: \qquad b = \frac{32\pi\epsilon\sigma^3}{63}\left[8\left(\frac{\sigma}{h}\right)^9 - 15\left(\frac{\sigma}{h}\right)^3\right]$$

$$BB: \qquad V_0 = \frac{33}{8}\left[\frac{b}{4\pi\sigma^3} + \frac{8}{9}\varepsilon\right]$$

$$OT: \qquad b = \frac{16\pi\epsilon\sigma^3}{9}\left[\left(\frac{\sigma}{h}\right)^9 - 3\left(\frac{\sigma}{h}\right)^3\right]$$

As this is an effective interaction, there is no fundamental reason for keeping the Lenard-Jones values for the He-He interaction ϵ=10.22 K and σ=2.556 Å, but this is a reasonable choice which restricts thus the number of adjustable parameters. In Fig. 8 are displayed these three effective potentials.

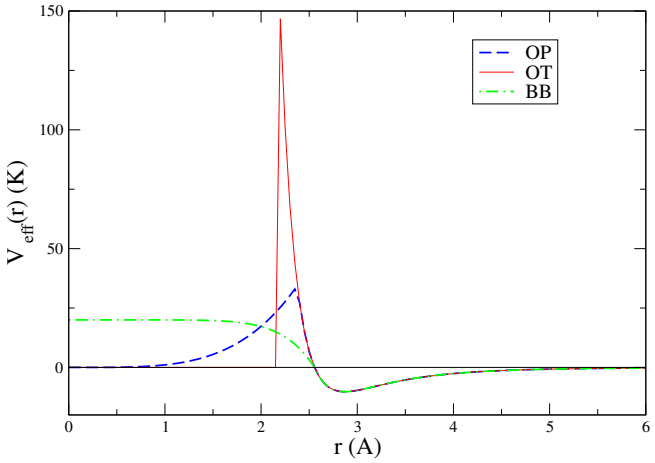

Figure 8: The three effective potentials $V_{\rm eff}(r)$ discussed in these notes.

At this stage, there is no *a priori* reason to prefer one of these effective potentials over the others. What matters is that all of them contain what we consider the basic features of a finite range interaction, namely an r^{-6} tail as well as a repulsion at short distances. However, we will see in Sec. 3.4 that the differences in the choice for $V_{\rm in}$ translates in momentum space, with sizeable consequences on dynamical effects as the response function.

In the zero-range ST functional, inhomogeneities in the density have been considered by means of a term $(\nabla\rho)^2$, depending on the density gradient. However, this approach is restricted to smooth inhomogeneities. Indeed, the density dependence ρ^γ of the repulsive $c-$term causes the density profile to stay smooth, as any deviation from an average density is energetically unfavorable. The alternative followed in Ref. [22] is to introduce non-local terms by means of a coarse-grained density $\tilde{\rho}(\mathbf{r})$, as suggested by Tarazona [26] in his study of classical fluids as a hard spheres system. The averaged density is defined as

$$\tilde{\rho}(\mathbf{r}) = \int d\mathbf{r}' w(\mathbf{r}-\mathbf{r}')\rho(\mathbf{r}') \tag{76}$$

where the weight function $w(r)$ has been taken as

$$\begin{aligned} w(r) &= \frac{3}{4\pi h'^3} \qquad r < h' \\ &= 0 \qquad\qquad \text{otherwise} \end{aligned} \tag{77}$$

This coarse-grained density $\tilde{\rho}(\mathbf{r})$ can be viewed as the mean density around a particle at $\mathbf{r}$, in a volume related to the range of the interaction. In this way, any narrow peak in the density $\rho(\mathbf{r})$ will be smeared out in $\tilde{\rho}(\mathbf{r})$. The value of parameter h' should be around the range of the interaction, i.e. of the order of the LJ parameter σ or the parameter h of the effective interaction (Eq. 72).

All in all, OP and BB functionals have the same form:

$$E[\rho] = \int d\mathbf{r} \left\{ \frac{\hbar^2}{2m} \left(\nabla \sqrt{\rho(\mathbf{r})} \right)^2 + \frac{1}{2} \int \mathrm{d}\mathbf{r}' \, V_{\text{eff}}(\mathbf{r} - \mathbf{r}') \rho(\mathbf{r}) \rho(\mathbf{r}') + \frac{1}{2} c \rho(\mathbf{r}) \tilde{\rho}^{1+\gamma}(\mathbf{r}) \right\} \tag{78}$$

only differing in the choice for V_{in}. Notice that for the homogeneous helium system (i.e. constant density), it reduces to the ST functional (64). The parameters are given in Table 4.

Table 4: Parameters of OP and BB functionals for ^{4}He systems.

ϵ (K)	σ (Å)	c (K Å$^{3(1+\gamma)}$)	γ	h (Å)	h' (Å)	V_0 (K)
10.22	2.556	1.04554×10^7	2.8	2.377	2.377	20.00

The exchange-correlation term of OT functional is a bit different:

$$\begin{aligned} E[\rho] \;=\; & \int d\mathbf{r} \left\{ \frac{\hbar^2}{2m} \left(\nabla \sqrt{\rho(\mathbf{r})} \right)^2 + \frac{1}{2} \int \mathrm{d}\mathbf{r}' V_{\text{eff}}(\mathbf{r} - \mathbf{r}') \rho(\mathbf{r}) \rho(\mathbf{r}') \right. \\ & + \frac{1}{2} c_2 \rho(\mathbf{r}) \tilde{\rho}^2(\mathbf{r}) + \frac{1}{3} c_3 \rho(\mathbf{r}) \tilde{\rho}^3(\mathbf{r}) \\ & \left. - \frac{\hbar^2}{4m} \alpha_s \int \mathrm{d}\mathbf{r}' F(\mathbf{r} - \mathbf{r}') \left(1 - \frac{\bar{\rho}(\mathbf{r})}{\rho_{0s}} \right) \nabla \rho(\mathbf{r}) \nabla' \rho(\mathbf{r}') \left(1 - \frac{\bar{\rho}(\mathbf{r}')}{\rho_{0s}} \right) \right\} \end{aligned} \tag{79}$$

It contains two integer powers of the coarse-grained density as well as a non-local correction to the kinetic energy, with coefficient α_s. It contains another averaged density $\bar{\rho}$, defined as

$$\bar{\rho}(\mathbf{r}) = \int d\mathbf{r}' F(\mathbf{r} - \mathbf{r}') \rho(\mathbf{r}') \tag{80}$$

with a weighting function

$$F(r) = \frac{1}{\pi^{3/2} \ell^3} \mathrm{e}^{-r^2/\ell^2} \tag{81}$$

where $\ell = 1$ Å. This term is crucial to reproduce the experimental static response function of the liquid [24].

For the homogeneous liquid, the OT functional leads to an energy per particle

$$\frac{E}{N} = \frac{1}{2} b\rho + \frac{1}{2} c_2 \rho^2 + \frac{1}{3} c_3 \rho^3 \tag{82}$$

depending on the three parameters b, c_2 and c_3. These are determined in a similar way as in the ST case. The parameters of the OT functional are given in Table 5.

Table 5: Parameters of the OT functional for ^{4}He systems (from Ref. [24]).

ϵ (K)	σ (Å)	h/σ	h'/σ
10.22	2.556	0.85692	0.85692
c_2 (K Å^6)	c_3 (K Å^7)	α_s (Å^3)	ρ_{0s} (Å^{-3})
-2.411857×10^4	1.858496×10^6	54.31	0.04

3.3 Free surface

An important subject in relation with quantum liquids is the study of their surface properties, as the surface tension and density profile. The surface tension of liquid helium has been accurately measured; at variance, the density profile is not, for the time being, experimentally accessible. Experimental determinations of the surface thickness (see Sec. 3.5) are available for helium films deposited on planar solid substrates [29].

Let us see how to determine the surface tension and density profile. The crucial point is to realize that there are two phases in equilibrium –liquid and vapor– having the same T and chemical potential, which are separated by an interface whose properties one wants to determine. Far from the interface one phase is the bulk liquid and the other a helium vapor; at $T = 0$, there is no vapor and the chemical potential is μ_0 (the $e_0 = -7.15$ K in Table 1).

The thermodynamic potential to minimize to determine the surface properties is thus the grand potential $E - \mu N$ with $\mu = \mu_0$:

$$E - \mu N = \int d\mathbf{r} \, \{\mathcal{E}[\rho, \nabla\rho] - \mu_0 \rho\} \tag{83}$$

where a contribution of $\nabla\rho$ type arise, at least, from the kinetic energy density. Without loss of generality, we can assume that the free surface of the liquid defines the plane (x, y). The liquid has translational invariance parallel to the free surface, and therefore the wave function of the system only depends on the coordinate z,

perpendicular to the (x, y)-plane. The density is only a function of z, being constant on planes perpendicular to the z-axis. The grand potential per unit surface is the surface tension, given by

$$\sigma = \frac{E - \mu N}{\Sigma} = \int_{-\infty}^{\infty} dz \, \{\mathcal{E}(\rho, \rho') - \mu_0 \rho\} \tag{84}$$

where $\mathcal{E}$ is the energy per unit of volume, and ρ' stands for the derivative with respect to z. The Euler-Lagrange equation reads

$$\frac{\delta}{\delta \rho(z)} \{\mathcal{E}[\rho(z), \rho'(z)]\} = \mu_0 \tag{85}$$

We can see the physical meaning of this equation: the equilibrium density profile minimizes the surface tension of the system. The solution of this equation gives the density profile $\rho(z)$ and the surface tension. The conditions imposed to the density profile are that when $r \to -\infty$, $\rho(z) \to \rho_0$, and that when $r \to \infty$, $\rho(z) \to 0$.

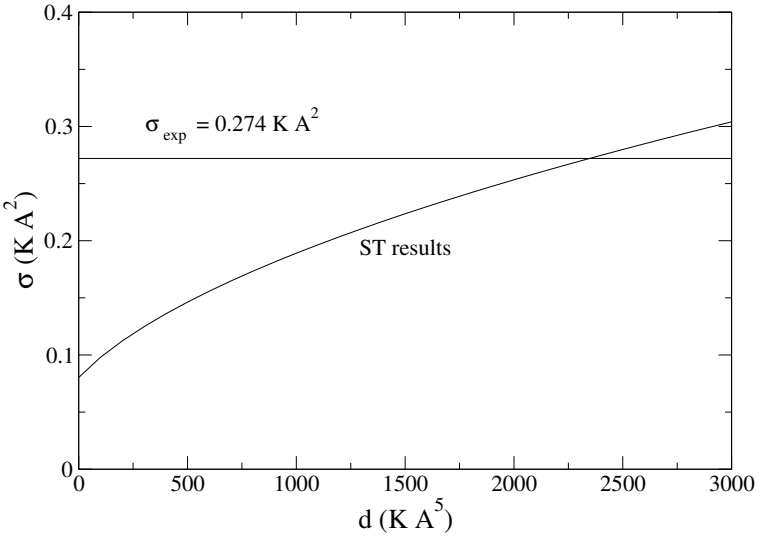

Figure 9: Surface tension as a function of parameter d, calculated with the ST density functional.

It is remarkable that for zero-range functionals of ST type containing a kinetic energy term proportional to $(\nabla\rho)^2/\rho$ and a surface energy term proportional to $(\nabla\rho)^2$, the surface tension can be determined, even a $T \neq 0$ [33], without solving the Euler-Lagrange equation. Actually, Eq. (84) can be written in that case as:

$$\sigma = 2 \int_0^{\rho_0} d\rho \left[(\frac{\hbar^2}{8m} + d\rho)(\frac{1}{2} b\rho + \frac{1}{2} c\rho^{1+\gamma} - \mu) \right]^{1/2} \tag{86}$$

This equation allows one to fix the still free parameter d of the ST functional (64). In Fig. 9 is represented the surface tension σ calculated with the ST density

functional as a function of parameter d, keeping the previously determined values of b, c and γ. The surface tension obtained for $d = 0$ (i.e. with the only inhomogeneities associated to the kinetic energy term) is 0.080 KÅ^{-2}, more than three times smaller than the experimental value $\sigma = 0.274$ KÅ^{-2}. This completes the determination of the ST density functional, whose parameters are given in Table 3.

Last but not least, let us mention that in the ST case the density profile –$z(\rho)$ rather than $\rho(z)$– can be easily obtained [33]

$$\int_{\rho_0/2}^{\rho(z)} d\xi \left[\frac{\frac{\hbar^2}{8m\xi} + d}{\frac{1}{2}b\xi^2 + \frac{1}{2}c\xi^{2+\gamma} - \mu_0\xi} \right]^{1/2} = z - z_0 \tag{87}$$

where arbitrarily the value z_0 has been chosen such that $\rho(z_0) = \rho_0/2$.

3.4 Dynamical properties

We have mentioned that zero-range functionals are not well adapted to situations where spatial variations come into play, and finite-range and non-local terms are necessary. The importance of these effects are manifested when trying to describe dynamical characteristics. We shall illustrate this point by looking at the zero sound dispersion relation in the bulk liquid.

The starting point is the particle-hole interaction as defined in Eq. (60). For the zero-range ST functional one gets

$$V_{ph}^{ST}(q) = b\rho + \frac{1}{2}(2+\gamma)(1+\gamma)c\rho^{1+\gamma} \tag{88}$$

which is independent of q. By contrast, finite-range functionals give rise to a momentum dependence. Specifically one obtains

$$V_{ph}^{OP}(q) = \rho\tilde{V}_{\rm eff}^{OP}(q) + \frac{1}{2}(1+\gamma)c\left[2\tilde{w}(q) + \gamma\tilde{w}^2(q)\right]\rho^{1+\gamma} \tag{89}$$

$$V_{ph}^{BB}(q) = \rho\tilde{V}_{\rm eff}^{BB}(q) + \frac{1}{2}(1+\gamma)c\left[2\tilde{w}(q) + \gamma\tilde{w}^2(q)\right]\rho^{1+\gamma} \tag{90}$$

$$V_{ph}^{OT}(q) = \rho\tilde{V}_{\rm eff}(q) + c_2\left[2\tilde{w}(q) + \tilde{w}^2(q)\right]\rho^2 + 2c_3\left[\tilde{w}(q) + \tilde{w}^2(q)\right]\rho^3 - \frac{\hbar^2}{2m}\alpha_s\rho\left(1 - \frac{\rho}{\rho_{0s}}\right)^2 q^2 {\rm e}^{-q^2l^2/4} \tag{91}$$

where $\tilde{w}(q)$ is the Fourier transform of the weight function entering the coarse grained density:

$$\tilde{w}(q) = \frac{3}{q^3h^3}\left(\sin qh' - qh'\cos qh'\right) \tag{92}$$

and $\tilde{V}_{\rm eff}(q)$ is the Fourier transform of the effective potential

$$\tilde{V}_{\rm eff}^{OP}(q) = 4\pi V_{LJ}(h)h^3 \int_0^1 dx \frac{\sin qhx}{qh} x^5 + f(q, h/\sigma) \quad (93)$$

$$\tilde{V}_{\rm eff}^{BB}(q) = 4\pi V_0 \sigma^3 \int_0^1 dx \frac{\sin q\sigma x}{q\sigma}(x - x^9) + f(q, 1) \quad (94)$$

$$\tilde{V}_{\rm eff}^{OT}(q) = f(q, h/\sigma) \quad (95)$$

where we have defined

$$f(q, a) = 16\pi\varepsilon\sigma^3 \int_a^\infty dx \frac{\sin q\sigma x}{q\sigma} \left(\frac{1}{x^{11}} - \frac{1}{x^5}\right) \quad (96)$$

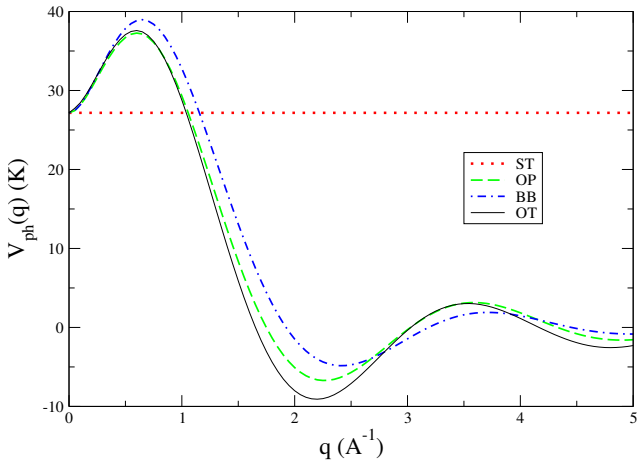

Figure 10: ^{4}He particle-hole interaction as calculated with several density functionals.

The particle-hole interactions corresponding to these functionals are plotted in Fig. 10 as a function of q. It is worth stressing that they look similar in the region $q \leq 0.7$ Å^{-1}. Beyond this value, the qualitative behavior is similar, but the different choices for the short-range term $V_{\rm in}$ reflect in quantitatively different particle-hole interactions. Let us now see how these different behavior translates into the dispersion relation $\varepsilon(q) = \hbar\omega(q)$. It is given by the poles of the real part of the response function. From Eqs. (56) and (58) one gets

$$\varepsilon(q) = \sqrt{\left(\frac{\hbar^2 q^2}{2m}\right)^2 + V_{ph}(q)\frac{\hbar^2 q^2}{m}} \quad (97)$$

We can see that the dominant term when $q \to 0$ is

$$\varepsilon(q) \to \hbar c q \quad (98)$$

where c is the speed of sound, since $V_{ph}(q) \to mc^2$ as $q \to 0$. This is the phonon region, which by construction, is well reproduced by any of these density functionals. In Fig. 11 are displayed the results obtained with ST, OP and BB functionals. Beyond the value $q \simeq 0.5$ Å^{-1}, the zero-range density ST predicts a q^2 behavior (not

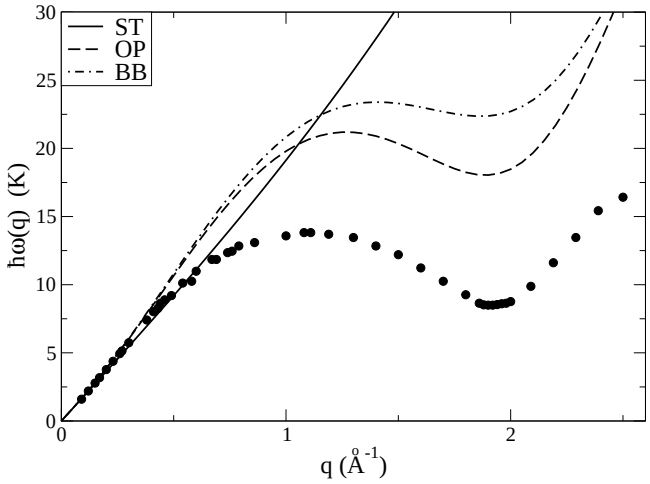

Figure 11: ^{4}He zero-sound dispersion relation at saturation, as calculated with ST, OP and BB density functionals.

easily seen at this scale), while the finite range OP and BB give only a qualitative account of the maxon and roton regions. More physics is required to reproduce them, as we discuss now in connection with OT functional.

The wave function of the condensate can be writen as

$$\Psi(\mathbf{r}) = |\Psi(\mathbf{r})|\mathrm{e}^{iS(\mathbf{r})} = \sqrt{\rho(\mathbf{r})}\mathrm{e}^{iS(\mathbf{r})} \tag{99}$$

Up to now we have been dealing with $\rho(\mathbf{r})$, and ignored the (real) phase $S(\mathbf{r})$. It plays however a major role in characterizing superfluid phenomena. In particular, the phase is an essential ingredient to describe quantized vortices, either in the bulk or in droplets. It is related to the current density, which is defined as

$$\mathbf{j}(\mathbf{r}) = \frac{\hbar}{2mi}\left(\nabla' - \nabla\right)\rho(\mathbf{r},\mathbf{r}')|_{\mathbf{r}'=\mathbf{r}} = \frac{\hbar}{2mi}[(\nabla\Psi)\Psi^* - \Psi(\nabla\Psi^*)] \tag{100}$$

which in general is different from zero if the wave function is not real. The current can also be written as

$$\mathbf{j}(\mathbf{r}) = \frac{\hbar}{m}\rho(\mathbf{r})\nabla S(\mathbf{r}) \equiv \rho(\mathbf{r})\mathbf{v}(\mathbf{r}) \tag{101}$$

where $\mathbf{v}(\mathbf{r})$ is the velocity of the fluid. It is zero in the case of ground state calculations, so that $E \equiv E[\rho]$, but in general one must take $\mathbf{j}$ (or $\mathbf{v}$) into account for dynamical calculations.

The OT functional given in Eq. (80) has been completed so as to include a velocity dependence:

$$\begin{aligned} E^{OT}[\rho,\mathbf{v}] &= \int d\mathbf{r}\left[\frac{\hbar^2}{2m}\left(\nabla\sqrt{\rho(\mathbf{r})}\right)^2+\frac{1}{2}m\rho(\mathbf{r})\mathbf{v}^2(\mathbf{r})\right] \\ &+ \frac{1}{2}\int\int d\mathbf{r}\,d\mathbf{r}'\rho(\mathbf{r})\rho(\mathbf{r}')V_{\rm eff}(\mathbf{r}-\mathbf{r}') \\ &+ \int d\mathbf{r}\left\{\frac{1}{2}c_2\rho(\mathbf{r})\tilde{\rho}^2(\mathbf{r})+\frac{1}{3}c_3\rho(\mathbf{r})\tilde{\rho}^3(\mathbf{r})\right\} \\ &- \frac{\hbar^2}{4m}\alpha_s\int d\mathbf{r}\int \mathrm{d}\mathbf{r}'F(\mathbf{r}-\mathbf{r}')\left(1-\frac{\bar{\rho}(\mathbf{r})}{\rho_{0s}}\right)\nabla\rho(\mathbf{r})\nabla'\rho(\mathbf{r}')\left(1-\frac{\bar{\rho}(\mathbf{r}')}{\rho_{0s}}\right) \\ &- \frac{1}{2}m\int\int d\mathbf{r}\,d\mathbf{r}'\rho(\mathbf{r})\rho(\mathbf{r}')V_J(\mathbf{r}-\mathbf{r}')|\mathbf{v}(\mathbf{r})-\mathbf{v}(\mathbf{r}')|^2 \end{aligned} \tag{102}$$

We identify the first line as the kinetic energy contribution, sum of the quantum zero-point motion plus the classical kinetic energy of a fluid. The next three lines contain the terms previously discussed of effective interaction and exchange-correlation effects. Together with the zero-point motion they are usually sufficient when considering ground state properties. The last line is a new term, which acts as a backflow and depends on ρ and $\mathbf{v}$. The word backflow was introduced by Feynman and Cohen [34] to describe the correlated motion of neighboring particles around a given reference atom. It contains an effective "current"-interaction V_J, whose form has to be guessed and whose parameters are fitted so as to reproduce the dispersion relation. In the bulk, its contribution to the bulk particle-hole interaction is

$$-\rho\frac{\hbar^2}{2m}\,q^2\,\left\{\hat{V}_J(0)-\hat{V}_J(q)\right\} \tag{103}$$

where $\hat{V}_J(q)$ is the Fourier transform of $V_J(r)$.

The OT choice is given by the following parameterization:

$$V_J(r)=(\gamma_{11}+\gamma_{12}r^2)\mathrm{e}^{-\alpha_1 r^2}+(\gamma_{21}+\gamma_{22}r^2)\mathrm{e}^{-\alpha_2 r^2} \tag{104}$$

with six parameters

$$\begin{array}{lll} \gamma_{11}=-19.7544 & \gamma_{12}=12.5616\ \text{Å}^{-2} & \alpha_1=1.023\ \text{Å}^{-2} \\ \gamma_{21}=-.2395 & \gamma_{22}=.0312\ \text{Å}^{-2} & \alpha_2=.14912\ \text{Å}^{-2} \end{array}$$

The resulting dispersion relation $\varepsilon(q)$ is plotted as a function of q in Fig. 12, calculated as indicated in Ref. [12]. The dots are the experimental data, and the

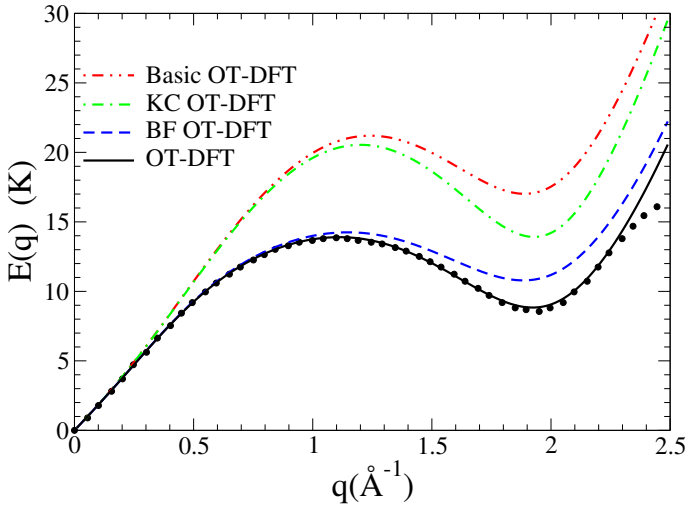

Figure 12: Dispersion relation for elementary excitations in liquid ^{4}He [2] as calculated with the OT functional at several levels of approximation.

solid line has been calculated with the full OT functional (102). In most time-dependent applications, both the non-local kinetic energy correlation [KC, fourth line in Eq. (102)] and backflow [BF, last line in Eq. (102)] terms are often neglected because their evaluation is time consuming and they tend to exhibit numerical instabilities, especially for highly inhomogeneous systems. They are however required to achieve the nice quantitative agreement showed in Fig. 12 with the experimenatl dispersion relation. To see their relative importance the figure displays also the results obtained dropping them in the following way: basic OT-DFT (KC and BF set to zero), KC OT-DFT (BF to zero), and BF OT-DFT (KC to zero). To reproduce the maxon-roton region, the BF term is absolutely necessary, the KC term being a relatively small correction.

3.5 Drops of ^{4}He

Once fixed energy functionals by fitting bulk properties, we consider now the predictions for droplets of ^{4}He atoms. Assuming these to have spherical symmetry, the KS equation writes

$$\left\{\frac{\hbar^2}{2m}\frac{d^2}{dr^2} + U_S(r)\right\}\left(r\sqrt{\rho(r)}\right) = \mu\left(r\sqrt{\rho(r)}\right) \tag{105}$$

This is an integro-differential equation, which is solved iteratively. An initial density profile is guessed to calculate the KS potential $U_S(r)$, given in Eq. (63), and obtain a new density profile, which is used to calculate a new KS potential and so on till some convergence criterium is reached. The density has to remain finite at the origin

and vanish for large values of r. Details how the KS equations are solved in practice can be found in Ref. [3].

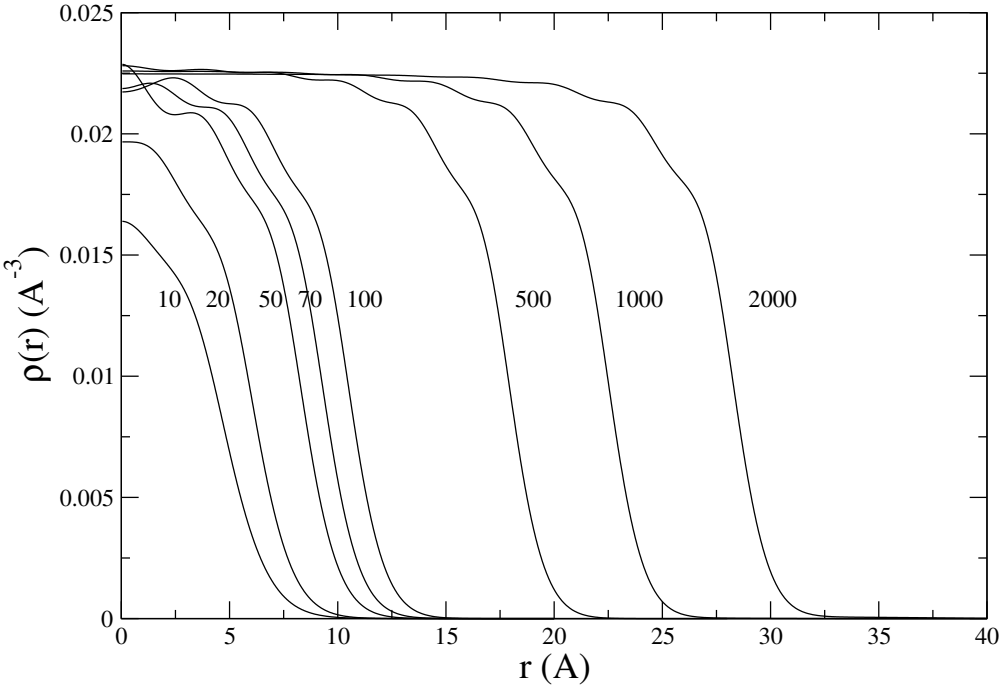

Figure 13: Density profiles for $^4\mathrm{He}_N$ drops, calculated with the OT density functional.

In Fig. 13 are shown the atom densities obtained with the OT functional for drops containing an increasing number of ^{4}He atoms from 10 to 2000. The most noticeable characteristics of these density profiles are the tendency of the central density to reach a central density ρ_c that gets closer and closer to the liquid density ρ_0 at saturation, together with a rather narrow surface region whose thickness also tends to that of the liquid helium free surface. This is a consequence of the fairly short-range of the atom-atom potential (much shorter than the $1/r$-dependence of the Coulomb or gravitational potential). Although the attractive part of the atom-atom interaction provides the binding mechanism, this binding is constrained by the repulsive core of the interaction. The repulsion defines a closest packing which applies to droplets of any size. In other words, the average distance between helium atoms is about the same in all droplets, and this then also holds true for the central density of droplets. This property is called *saturation*. It has consequences on the binding energy per atom (see below), and on the spatial distribution of the density inside a droplet which basically becomes constant inside. These arguments are generic for all saturating systems as classical liquids, valence electrons in metal clusters or nucleons in atomic nuclei.

A striking feature of the density profiles is the presence of noticeable oscillations.

They are are absent when one uses a zero-range functional as ST, and are thus related to some of the characteristics of the OT functional, as e.g. its finite range, but not only [24]. In particular, the oscillations are much depressed if the non-local kinetic energy term (α_s term in Eq. (80)) is not considered.

In Fig. 14 are compared, for small droplets, the density profiles yielded by a DMC calculation with those obtained using the OT functional. We can observe that the overall agreement is excellent. Notice that only experimental information on the bulk liquid has been used to adjust the free parameters of the OT functional.

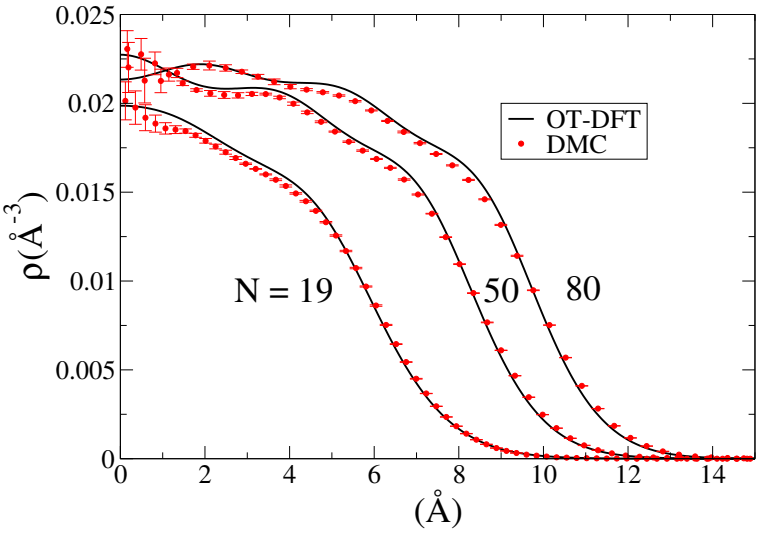

Figure 14: Density profiles for ^4He_N droplets calculated within a diffusion Monte Carlo method (M. Rossi, U. of Padova) and using the OT density functional (M. Pi, U. of Barcelona).

The saturation property also manifests in terms of the drops size. Indeed, the volume of the droplet is roughly proportional to the number of atoms N, and its size is proportional to $N^{1/3}$. From the mean-square radius

$$\langle r^2 \rangle = \frac{4\pi}{N} \int_0^\infty dr\, r^4\, \rho(r) \tag{106}$$

one defines the unit radius

$$r_0 = \sqrt{\frac{5}{3}\langle r^2 \rangle} N^{-1/3}$$

In Table 6 are displayed the central density $\rho_c = \rho(r = 0)$, the unit radius r_0 and the surface thickness t, defined as the difference between radii values where the density has decreased from its central value ρ_c by 10% and by 90%, i.e. $t = r(\rho = 0.1\rho_c) - r(\rho = 0.9\rho_c)$. Experimental values for ^{4}He films on Si wafers at $T = 0.45$ K are in the 5.3-6.5 Å range depending on the film thickness [29].

Table 6: Unit radius r_0 (Å), central density ρ_c (Å^{-3}) and thickness t (Å) for $^4\mathrm{He}_N$ droplets, calculated with ST and OT functionals. The DMC results are from Refs. [27, 28].

N	ST			OT			DMC
	r_0	ρ_c	t	r_0	ρ_c	t	r_0
8	4.19	0.0076	6.6	3.10	0.0145	4.2	3.20
10	3.83	0.0095	6.8	3.05	0.0164	4.9	3.07
20	3.10	0.0161	6.8	2.70	0.0197	5.3	2.74
40	2.73	0.0205	6.9	2.51	0.0212	5.3	2.58
70	2.56	0.0222	7.2	2.42	0.0219	5.4	2.42
112	2.47	0.0228	7.4	2.37	0.0225	5.6	2.39
240	2.36	0.0230	7.4	2.31	0.0227	5.6	
330	2.33	0.0230	7.3	2.29	0.0226	5.6	
728	2.28	0.0228	7.2	2.26	0.0226	5.6	
1000	2.27	0.0227	7.2	2.25	0.0226	5.7	
2000	2.25	0.0225	7.1	2.24	0.0225	5.7	
...							
bulk	2.22	0.0218	~ 7 [24]	2.22	0.0218	~ 6 [24]	

For large droplets, the central density ρ_c should approach the value for the bulk liquid ρ_0 in Table 1; similarly, the unit radius should approach the bulk radius r_0 (or Wigner-Seitz radius) defined from $4\pi r_0^3\rho_0/3 = 1$, that yields $r_0 = 2.22$ Å. It can be seen that the bulk liquid values are reached rather slowly when the number N of atoms in the drop increases. A useful quantity is the droplet sharp radius R_s, defined as $R_s = r_0 N^{1/3}$; a droplet of constant density ρ_0 and radius R_s contains N atoms.

The ST functional yields more diffuse densities, as compared to OT functional, whose unit radii are in close agreement with those obtained within DMC. We have not displayed DMC central densities because they are ill-defined due to the fairly large statistical errors, see Fig. 14. Neither the thickness can be unambiguously defined. Note that the appearance of a structured density profile at the surface (see Fig. 13) makes also difficult to define a surface thickness t in the case of a finite-range functional.

Let us now discuss the droplet energies. In general, one expects that for an ensemble of N particles interacting with a long-range interaction, the potential energy is proportional to the number of pairs of interacting particles, namely $N(N-1)/2$ which is about N^2 for large values of N. However, owing to the short range atom-atom interaction, a given atom only interacts with its closest neighbors. This property allows one to deduce the useful "liquid-drop formula". In the bulk liquid, the

energy is only proportional to N, and not to the total number of pairs: $E = -a_{\rm v}N$, where the positive quantity $a_{\rm v}$ is referred to as "volume" coefficient. In the case of droplets, this is a rough estimate because an atom at the surface of the droplet interacts with less atoms than when it is in its bulk. The surface then induces a correction to the volume contribution which has an opposite sign. As the size scales as $N^{1/3}$, the surface scales as $N^{2/3}$. The net result is a (positive) surface correction term of the form $a_{\rm s}N^{2/3}$. Including more corrections one writes the liquid drop formula, giving the energy as an expansion in decreasing powers of $N^{-1/3}$. Only the first 3-4 terms are relevant. The energy per particle is thus written as

$$\frac{E}{N} = -a_v + a_s N^{-1/3} + a_c N^{-2/3} + a_0 N^{-1} + ... \tag{107}$$

This liquid drop formula is characteristic of saturating systems, with a volume term a_v (or bulk binding energy per particle), a surface term a_s (whose minimization determines the density profile of the free surface as we have seen), a curvature term a_c, etc.

Table 7: Energies per particle E/N (in K) for several $^4{\rm He}_N$ droplets. The DMC results are from Refs. [27, 28].

N	ST	OT	DMC
8	-0.390	-0.527	-0.640
10	-0.547	-0.784	-0.864
20	-1.257	-1.609	-1.697
40	-2.178	-2.491	-2.578
70	-2.926	-3.169	-3.253
112	-3.503	-3.690	-3.780
240	-4.307	-4.423	
330	-4.594	-4.689	
728	-5.193	-5.251	
1000	-5.393	-5.438	
2000	-5.762	-5.780	
...			
bulk	-7.15	-7.15	-7.15

In Table 7 are collected some results for the energies per particle as a function of the number of atoms in the drop. These have been obtained from the zero-range ST and finite-range OT functionals. Column labelled DMC shows diffusion Monte Carlo results using the Aziz atom-atom interaction HFD-B(HE) of Ref. [13] taken from Refs. [27, 28]. Notice that, within DFT, the droplets are less bound than within DMC. The DMC results are taken as the "experimental" ones, in the absence of experimental measurements for finite clusters. The overall agreement obtained

between microscopic and density functional calculations is striking. Recall that the DF parameters have been fitted so as to reproduce some selected properties of the homogeneous liquid at saturation, as well as the surface tension for ST, but not for OT. Consequently, the OT-DFT predictions for finite droplets are parameter-free.

The energies in Table 7 are represented in Fig. 15 as a function of $N^{-1/3}$. A

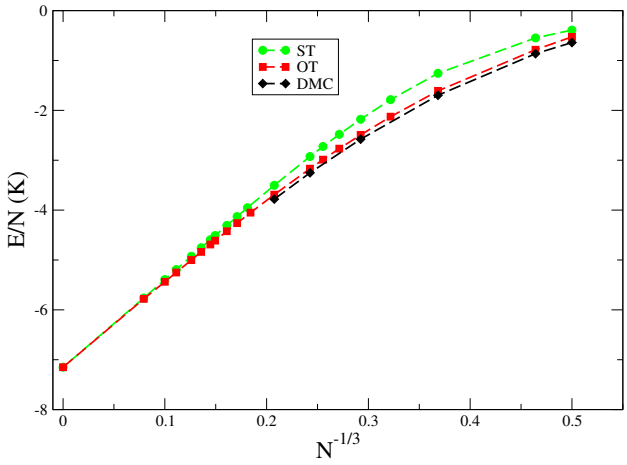

Figure 15: The energies per particle (in K) of Table 7 are plotted as a function of $N^{-1/3}$. The bulk value has also been included in the ST and OT cases.

fit of these values to the liquid-drop mass formula Eq. (107) yields the following expression for the energies per atom

$$\text{ST}: \quad \frac{E}{N} = -7.15 + 17.02N^{-1/3} + 9.76N^{-2/3} - 33.66N^{-1} \quad \text{(K)}$$

$$\text{OT}: \quad \frac{E}{N} = -7.15 + 17.56N^{-1/3} - 1.03N^{-2/3} - 15.29N^{-1} \quad \text{(K)}$$

In these expressions, the bulk energy per atom has been fixed to the experimental value (used in the fit of the ST and OT functionals).

Both functionals yield similar values for a_s (the slope of the E/N curves in Fig. 15 at the origin), related to the surface tension as $a_s = 4\pi r_0^2 \sigma$. Taking for $r_0 = 2.22$ Å, the "experimental" surface energy is $a_s = 16.97$ K. The surface tensions deduced from the fits above are 0.275 and 0.284 K Å^2 for ST and OT functionals, respectively; recall that the surface tensions, directly calculated from a planar liquid helium surface, are 0.274 (ST) and 0.272 K Å^2 (OT) [24]. As for a_v, one might have fixed a_s to the ST or OT value and only use the a_c and a_0 as fit parameters.

It is worth noticing that a relatively large range of N-values is required to obtain an accurate mass formula. Just as an example, the mass-formula fit to the DMC energies yields

$$\text{DMC}: \quad \frac{E}{N} = -7.59 + 21.10N^{-1/3} - 12.32N^{-2/3} - 41.16N^{-1} \quad \text{(K)}$$

where, at variance with the functional expressions above, the volume energy coefficient a_v has been let free in the fit. Interestingly, fixing a_v leads to a fit in closer agreement with ST and OT

$$\text{DMC}: \qquad \frac{E}{N} = -7.15 + 17.03N^{-1/3} - 0.332N^{-2/3} - 15.37N^{-1} \quad \text{(K)}$$

The interested reader is referred to Refs. [1, 2] for a thorough presentation of the properties of doped droplets. In these references one may also find a detailed account of the properties of mixed helium droplets, and of helium droplets hosting vortex lines.

Acknowledgments

J.N. has been supported by grant FIS2014-51948-C2-1-P, Mineco (Spain), and M.B. by grants No. FIS2014-52285-C2-1-P, Mineco (Spain), and 2014SGR401 from Generalitat de Catalunya. MB also thanks the Université Fédérale Toulouse Midi-Pyrénées for financial support through the "Chaires d'Attractivité 2014" Programme IMDYNHE.

References

[1] M. Barranco, R. Guardiola, S. Hernández, R. Mayol, J. Navarro, and M. Pi, *J. Low Temp. Phys.* **142**, 1 (2006).

[2] F. Ancilotto, M. Barranco, F. Coppens, J. Eloranta, N. Halberstadt, A. Hernando, D. Mateo, and M. Pi, *Int. Rev. Phys. Chem., to be published 2017-18*

[3] M. Barranco, F. Coppens, N. Halberstadt, A. Hernando, A. Leal, D. Mateo, R. Mayol, and M. Pi, *Zero temperature DFT and TDDFT for ^{4}He: A short guide for practitioners* (2017), https://github.com/bcntls2016/DFT-Guide/blob/master/dft-guide.pdf.

[4] J. Wilks and D.S. Betts, *An Introduction to Liquid Helium* (Clarendon Press, Oxford, 1987).

[5] H.R. Glyde, *Excitations in Liquid and Solid Helium* (Clarendon Press, Oxford, 1994).

[6] *Microscopic approaches to quantum liquids in confined geometries*, edited by E. Krotscheck and J. Navarro (World Scientific, Singapore, 2002).

[7] E.R. Dobbs, *Helium three* (Oxford U. Press, New York, 2000).

[8] P. Hohenberg and W. Kohn, *Phys. Rev.* **B136**, 864 (1964).

[9] W. Kohn and L.J. Sham, *Phys. Rev.* **140**, A1133 (1965).

[10] R.M. Dreizler and E.K.U. Gross, *Density Functional Theory. An Approach to the Quantum Many-Body Problem* (Springer-Verlag, Berlin, 1990).

[11] R.J. Donnelly and C.F. Barenghi, *J. Phys. Chem. Ref. Data* **27**, 1217 (1998).

[12] D. Mateo, M. Barranco, and J. Navarro, *Phys. Rev. B* **82**, 134529 (2010).

[13] R.A. Aziz, F.R.W. McCourt, and C.C.K. Wong, *Mol. Phys.* **61**, 1487 (1987).

[14] R.E. Grisenti, W. Schöllkopf, J.P. Toennies, G.C. Hegerfeldt, T. Khler, and M. Stoll, *Phys. Rev. Lett.* **85**, 2284 (2000).

[15] L. Pitaevskii and S. Stringari, *Bose-Einstein Condensation* (Clarendon Press, Oxford 2003).

[16] S. Grebenev, J. P. Toennies, and A. Vilesov, Science **279**, 2083 (1998).

[17] J.P. Toennies, A.F. Vilesov, and K.B. Whaley, *Phys. Today*, February 2001, 31.

[18] S. Stringari, *Phys. Lett. A* **106**, 267 (1984).

[19] Y.M. Engel, D.M. Brink, K. Goeke, S.J. Krieger, and D. Vautherin, *Nucl. Phys. A* **249**, 215 (1975).

[20] S. Stringari and J. Treiner, *J. Chem. Phys.* **87**, 5021 (1987).

[21] M.A. Solís and J. Navarro, Phys. Rev. B **45**, 13080 (1992).

[22] J. Dupont-Roc, M. Himbert, N. Pavloff, and J. Treiner, *J. Low Temp. Phys.* **81**, 31 (1990).

[23] M. Barranco and E.S. Hernández, *Phys. Rev. B* **49**, 12078 (1994).

[24] F. Dalfovo, A. Lastri, L. Pricaupenko, S. Stringari and J. Treiner, *Phys. Rev. B* **52**, 1193 (1995).

[25] C.H. Aldrich III and D.M. Pines, *J. Low Temp. Phys.* **25**, 677 (1976); C.H. Aldrich III, C.J. Pethick and D.M. Pines, *J. Low Temp. Phys.* **25**, 691 (1976); C.H. Aldrich III, C.J. Pethick and D.M. Pines, *Phys. Rev. Lett.* **37**, 845 (1976); C.H. Aldrich III and D.M. Pines, *J. Low Temp. Phys.* **32**, 689 (1978).

[26] P. Tarazona, *Phys. Rev. A* **31**, 2672 (1983).

[27] M. Lewerenz, *J. Chem. Phys.* **106**, 4596 (1997).

[28] K.B. Whaley, *Int. Rev. Phys. Chem.* **13**, 41 (1994); K.B. Whaley, in *Advances in Molecular Vibrations and Collision Dynamics*, edited by J.M. Bowman and Z. Bacic (JAI Press, Greenwich, Conn., 1998), Vol. III, p. 397.

[29] K. Penanen, M. Fukuto, R.K. Heilman, I.F. Silvera, and P.S. Pershan, *Phys. Rev. B* **62**, 9621 (2000).

[30] E. Lipparini, *Modern Many-Particle Physics* (World Sci., Singapore 2003)

[31] L. Szybisz and I. Urrutia, *Phys. Lett. A* **338**, 155 (2005).

[32] M. Barranco, E.S. Hernández, R. Mayol, J. Navarro, M. Pi, and L. Szybisz, AIP Conf. Proc. **850** *Low Temp. Phys: LT24*, p. 149 (2006).

[33] A. Guirao, M. Centellas, M. Barranco, M. Pi, A. Polls, and X. Viñas, *J. Phys. Cond. Matt.* **4**, 667 (1992).

[34] R.P. Feynman and M. Cohen, *Phys. Rev.* **102**, 1189 (1956).